Naval Surface Warfare Center
Carderock Division
West Bethesda, MD 20817-5700

Experiment to Characterize Sea Fighter FSF-1 Wave Slamming

by

Lisa M. Minnick

Thomas C. Fu

Anne M. Fullerton

Kirk Anderson

Don C. Walker

20071128065

REPORT DOCUMENTATION PAGE

1. REPORT DATE (DD-MM-YYYY) June 2007	2. REPORT TYPE Final	3. DATES COVERED (From - To) 2/2006 – 3/2007

4. TITLE AND SUBTITLE	5a. CONTRACT NUMBER
Experiment to Characterize Sea Fighter FSF-1 Wave Slamming	N0001406WX20691
	5b. GRANT NUMBER
	5c. PROGRAM ELEMENT NUMBER

6. AUTHOR(S)	5d. PROJECT NUMBER
Lisa Minnick, Thomas C. Fu, Anne M. Fullerton, Kirk Anderson, Don C. Walker	5e. TASK NUMBER
	5f. WORK UNIT NUMBER 06-1-5600-452,-453,-454,-455

7. PERFORMING ORGANIZATION NAME(S) AND ADDRESS(ES) AND ADDRESS(ES)	8. PERFORMING ORGANIZATION REPORT NUMBER
Naval Surface Warfare Center Carderock Division 9500 Macarthur Boulevard West Bethesda, MD 20817-5700	NSWCCD-50-TR-2007/030

9. SPONSORING / MONITORING AGENCY NAME(S) AND ADDRESS(ES)	10. SPONSOR/MONITOR'S ACRONYM(S)
Attn: ONR Code 331 Chief of Naval Research Arlington, VA 22217-5660	ONR
	11. SPONSOR/MONITOR'S REPORT NUMBER(S)

12. DISTRIBUTION / AVAILABILITY STATEMENT
Approved for Public Release; Distribution Unlimited.

13. SUPPLEMENTARY NOTES

14. ABSTRACT

This report describes the data obtained from a field experiment to obtain full-scale qualitative and quantitative wave slamming data of the *Sea Fighter (FSF-1)*, a high-speed experimental vessel developed by the Office of Naval Research. A 4-day trial from April 18-21, 2006 was conducted which began in Port Angeles, WA and ended in San Diego, CA. This data includes measurement of the ambient environmental conditions (wind and waves) in which the ship was operating, including the incident waves impacting the vessel, ship motions (including accelerations and angular rates), and visual documentation of the wave field surrounding the ship. This data will be used in the development and validation of computational tools used for design and evaluation of high-speed ships.

15. SUBJECT TERMS

16. SECURITY CLASSIFICATION OF:			17. LIMITATION OF ABSTRACT	18. NUMBER OF PAGES	19a. NAME OF RESPONSIBLE PERSON Thomas Fu
a. REPORT UNCLASSIFIED	b. ABSTRACT UNCLASSIFIED	c. THIS PAGE UNCLASSIFIED		51	19b. TELEPHONE NUMBER (include area code) 301-227-7058

THIS PAGE INTENTIONALLY LEFT BLANK

CONTENTS

FIGURES

APPENDIX B

APPENDIX C

TABLES

ABSTRACT

This report describes the data obtained from a field experiment to obtain full-scale qualitative and quantitative wave slamming data of the *Sea Fighter (FSF-1)*, a high-speed experimental vessel developed by the Office of Naval Research. A 4-day trial from April 18-21, 2006 was conducted which began in Port Angeles, WA and ended in San Diego, CA. These data include measurement of the ambient environmental conditions (wind and waves) in which the ship was operating, including the incident waves impacting the vessel, ship motions (including accelerations and angular rates), and visual documentation of the wave field surrounding the ship. These data will be used in the development and validation of computational tools used for design and evaluation of high-speed ships.

ADMINISTRATIVE INFORMATION

INTRODUCTION

A specific need exists for a high-speed sealift (HSSL) capability that will allow forces to deploy rapidly from CONUS (Continental United States) to foreign ports. These HSSL vessels are projected to carry a payload of between 3500 and 4000 tons and operate at sustained speeds on the order of 43 knots or more, with a range of at least 5000 nautical miles. Adding to the technical challenge posed by this speed and endurance requirement is the fact that foreign ports are likely to be relatively small and undeveloped, requiring that the ships be relatively short and of relatively shallow draft. Together these requirements suggest that the resulting ships would need to be unconventional multihull vessels. The development of design tools and the accompanying test instrumentation for high-speed ships is of major impact to the Navy. Experimental model data exists for Sea Fighter, however the ability to understand, predict, and simulate the behavior of full-scale high-speed Navy ships is dependent upon acquiring full-scale data for both physical understanding and validation of predictive tools.

The development of computational tools used for HSSL ships requires specific data for validation. These HSSL design tools specifically address the vessel's performance and loading. Deterministic models of the sea surface in time and space are growing in their maturity and complexity, as are vessel motion prediction codes. Because very little, if any, full-scale field data exists for ships of this type traveling at high speeds, the primary objective of this work is to obtain full-scale qualitative and quantitative wave slamming data of the *Sea Fighter*. These data will include measurements of the ambient environmental conditions (wind and waves), the incident waves impacting the vessel, ship motions, including accelerations and angular rates, and visual documentation of the

free-surface/wave field surrounding the ship. Associated with these measurement objectives are accompanying instrumentation development objectives to insure the primary objectives can be met. Critical to improving the prediction of motion dynamics and vessel loading of full-scale vessels, is an ability to measure the ambient surface wave field in and around an underway vessel. An increasing knowledge gap exists in the ability to accurately measure the surface wave field from an underway vessel for analysis of hull motions and structural response.

During the trial from April 18-21, 2006 several underway wave measurement systems were deployed from *Sea Fighter* to allow the measurement of the surface wave field. These systems included an array of ultrasonic wave height sensors, a stereophotographic-based system, and systems utilizing a combination of electro-optical and electromagnetic sensors. Additionally, inertial and Global Positioning System (GPS) motion sensors were used for the evaluation of slamming loads measured onboard the *Sea Fighter* under a range of vessel speeds and sea states. The data will be used to provide benchmarks to the existing numerical codes, indicate gaps of understanding which require further research in our understanding of wave physics and ship motion, and provide tools for designing active control systems on high-speed, full scale ships.

FIELD EXPERIMENT DESCRIPTION

The *Sea Fighter* (see Figure 1 and Figure 2) is a high-speed experimental vessel, developed by the Office of Naval Research. Ship details are listed in Table 1. Christened in 2005, she is an aluminum catamaran with both diesel engines and gas turbines. Utilizing diesel engines she is capable of +20 knots. Utilizing gas turbines the ship is capable of +50 knots in calm seas. The *Sea Fighter* has four steerable Kamewa water jets. Additionally, the *Sea Fighter* has an installed "science package" of strain gauges, accelerometers, pressure gauges, and underwater viewing windows. The *Sea Fighter* was tested 18-21 April 2006 during a transit from Port Angeles, WA to San Diego, CA. Figure 3 shows a rough sketch of the course taken during the trial. The half circle and rectangular path shown south of the Oregon/California border was conducted for the purpose of collecting data at a variety of headings relative to the waves. These data were part of rough water seakeeping testing and will not be discussed in this report. Maneuvering and seakeeping data from this trial and previous trials were documented by NSWCCD, Code 5500.

Wave Field Characterization

To provide suitable validation data on full-scale wave slamming, the incoming wave must be characterized. The focus of this task was the characterization of the impacting waves, by utilizing LIDAR (Light Imaging Detection and Ranging), stereophotography, an array of acoustic sensors, and standard video cameras (for qualitative observations). This task included developing and carrying out onboard measurements of the incoming wave field in the bow region of the *Sea Fighter* using the various measurement systems. Both a scanning LIDAR system and a point measurement LIDAR system were used. The scanning system was utilized to make scans in multiple orientations to the wave field, but not simultaneously. Simultaneous measurements were made with the point measurement system. The stereo-optic system was used to provide

2

wave amplitudes of the incoming wave field through the use of a calibrated multiple-view camera system. An array of thirteen acoustic sensors provided point measurements of the near-field free surface. Nine standard video cameras were used for qualitative observations and were mounted in the same general locations as the acoustic sensors. The only wave field characterization data that will be discussed in this report is the data collected by the thirteen acoustic sensors and on-board video cameras.

Figure 1. Photograph of *Sea Fighter*.
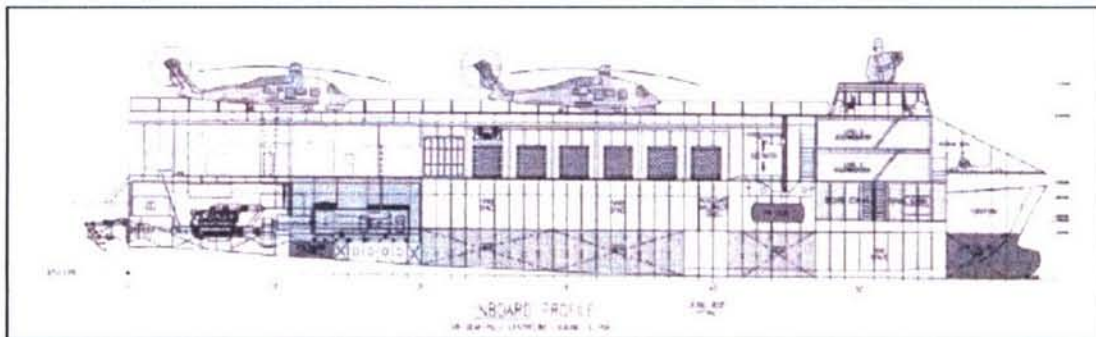
Figure 2. Ship drawing of *Sea Fighter*.

3

Figure 3. *SeaFighter* course during trial.

Table 1. *Sea Fighter* Hull Form Characteristics.

Ship Characteristics		
LOA	79.9 m	262 ft
LWL	73 m	240 ft
Beam	22 m	72 ft
Draft	3.5 m	11.5 ft
Displacement	960 metric tons	
Max Speed	50+ knots	
Max Speed (SS4)	40+ knots	
Range	> 4000 nm at 20 knots	

4

Underway Cameras

An array of nine cameras was deployed to provide qualitative support to the wave measurements. Seven cameras were mounted around the bow of the ship and two more cameras were deployed at the stern (from each hull, looking aft). The cameras were standard color video cameras in waterproof housing operating at 30 frames per second. Figure 4 shows the locations of the bow cameras and Figure B1 - Figure B5 in Appendix B provides details of the camera views.

Senix Ultrasonic Wave Height Sensors

Thirteen Senix ToughSonic distance sensors were used to measure the level of the free-surface at various locations around the vessel. An ultrasonic wave height transducer emits and receives the reflection of an acoustic signal. The time between the emission and receipt of the pulse allows for the calculation of the distance between the probe and the free-surface of the water. The probes have a 15 degree spread angle, meaning they average the signal received from a rather large patch of water, depending on the distance to the water surface itself. The sensors on board the *Sea Fighter* were mounted approximately 15-20 ft from the water surface. The sensors have a 10 Hz sampling rate, a range of 10 in to 30 ft, with an accuracy of 0.05 in. Figure 4 shows the location of the underway cameras and ultrasonic sensors, which were collocated at each of seven locations around the bow of the vessel. Table 2 lists the longitudinal and transverse locations of the bow sensors relative to the forward most bulkhead and vessel centerline. Sensors 3, 4, 6, and 7 and their associated cameras were mounted in the forward anchor wells as shown, while the remaining sensors were mounted off booms from the forecastle deck. Four additional sensors were deployed around the stern (two at the front of the boat ramp in the tunnel and two at the aft end). Data from the sensors and cameras were collected the entire time the ship was at sea.
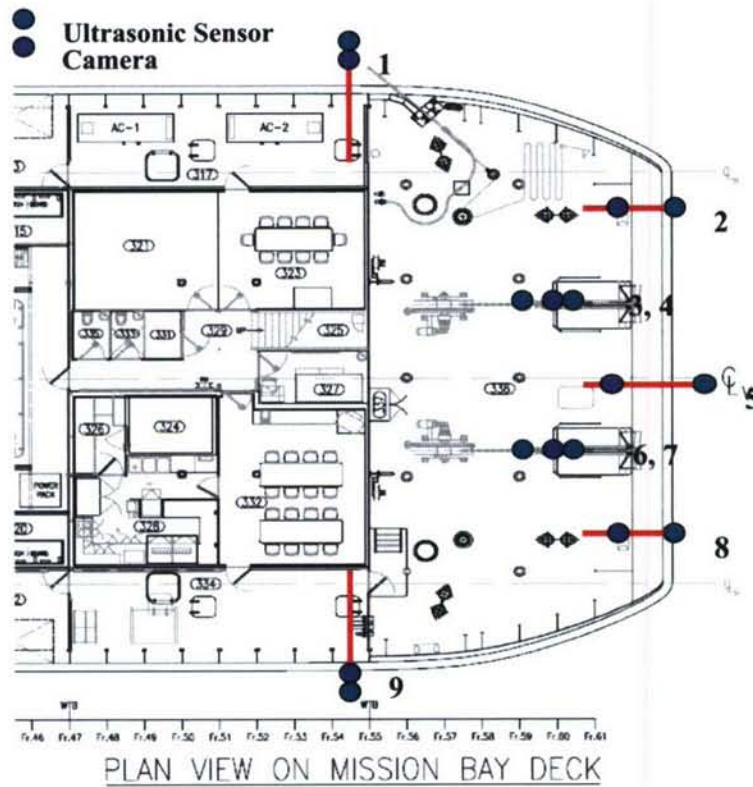
Figure 4. Diagram of bow ultrasonic and camera locations.

Table 2. Locations of Bow Ultrasonic Sensors.

Ultrasonic Senors		Longitudinal* Distance (ft)		Transverse Distance (ft)	
Port	1	3.42	Fwd BHD	37.74	Port CL
Port Bowline	2	33.44	Fwd BHD	19.34	Port CL
Port Fwd Anchor	3	29.09	Fwd BHD	7.18	Port CL
Port Aft Anchor	4	23.63	Fwd BHD	7.18	Port CL
Center	5	35.23	Fwd BHD	1.71	Stbd CL
Stbd Fwd Anchor	6	28.96	Fwd BHD	7.18	Stbd CL
Stbd Aft Anchor	7	23.50	Fwd BHD	7.18	Stbd CL
Stbd Bowline	8	33.65	Fwd BHD	19.42	Stbd CL
Stbd	9	3.92	Fwd BHD	37.99	Stbd CL

* referenced BHD is BHD at frame 55 (see Figure 4)

Scanning Laser Altimeter System (LIDAR)

The Scripps Scanning Laser Altimeter System is designed for accurate measurement of the water's free surface and is composed of three separate LIDAR units that operate in the near-infrared and have accuracies of a few centimeters. Two two-dimensional (2D) scanning LIDARs, the Riegl LMS-Q140i-80, and Riegl LMS-Q240-60, scanned the water surface forward of the *Sea Fighter* in two orthogonal planes. Each LIDAR had a motion package mounted with it to determine its orientation. A third, single-point LIDAR unit (Riegl LD90-3800EHS-FLP) was positioned to provide single point time series of the water elevation forward of the *Sea Fighter*. The horizontal scanning LIDAR unit (LMS-Q140i-80) was mounted to a Quickset QPT-90 software-controlled pan/tilt unit to allow at-sea adjustment of how far forward the system looked. Each LIDAR unit was mounted to a single tower deployed near the bow of the *Sea Fighter*. The LIDAR sweep rate was a minimum of 20 Hz, resulting in a cross-track resolution of approximately 1 m (40 Hz = 0.5 m resolution). Sweep rates, ping rates, and look angles of the LIDAR sensors were adjusted while at sea to return and optimize cross-track and along track resolutions of the surface wave measurements.

The forward LIDAR tower was 20 ft in length and was comprised of standardized 55G steel radio mast sections. It was located as far forward as possible onboard on the *Sea Fighter* to provide the necessary look angles for operation of the fixed and scanning LIDAR units. It stood approximately 35 ft above the water surface. The tower was mounted to the anchor deck directly underneath the forward hatch opening (near the flagpole). This location was required to allow the measurement of the free-surface as close as possible to the ship's bow (Figure 5 and Figure 6). The hatch is very near the centerline of the vessel. The tower also had guy wires to existing tie down points located on the *Sea Fighter*. A 2 ft x 2 ft 6061 AL baseplate was welded to the anchor deck directly beneath the hatch opening to provide a secure mount for the tower. The LMS-Q140 LIDAR was mounted on top of a pan/tilt unit at the top of the tower. The pan/tilt unit controlled the orientation of the LIDAR and could be operated remotely. The LIDAR was oriented to scan a swath parallel to the ship's bow (Figure 7); it was tilted 30 degrees downward such that it could see the free-surface, approximately 15 ft forward of the bow. The swath width was approximately 69 ft; the spatial resolution was 1 in. The second LIDAR, LMS-Q240, was mounted below the LMS-Q140, and fixed such that its swath was perpendicular to the bow and tilted approximately 45 degrees downward (Figure 8), and the swath width was 111 ft. The spatial resolution was 0.2 in. The tower also contained the third LIDAR unit, LD90-3800EHS-FLP, which provided a single point measurement. It was tilted approximately 13 degrees downward from vertical and had a spatial resolution of 2 in. The system was operated to provide single point time series of water surface elevation forward of the vessel, at the centerline. Figure 9 shows a photograph of the LIDAR tower on the *Sea Fighter*. Figure 10 illustrates the locations of the LIDAR and WaMoS towers. The data collected by the LIDAR system were not collected by NSWCCD and therefore will not be discussed in this report.

Figure 5. View of the *Sea Fighter* hatch opening at the bow.
The forward LIDAR tower was mounted to the anchor deck beneath the hatch, and
extended out its opening.
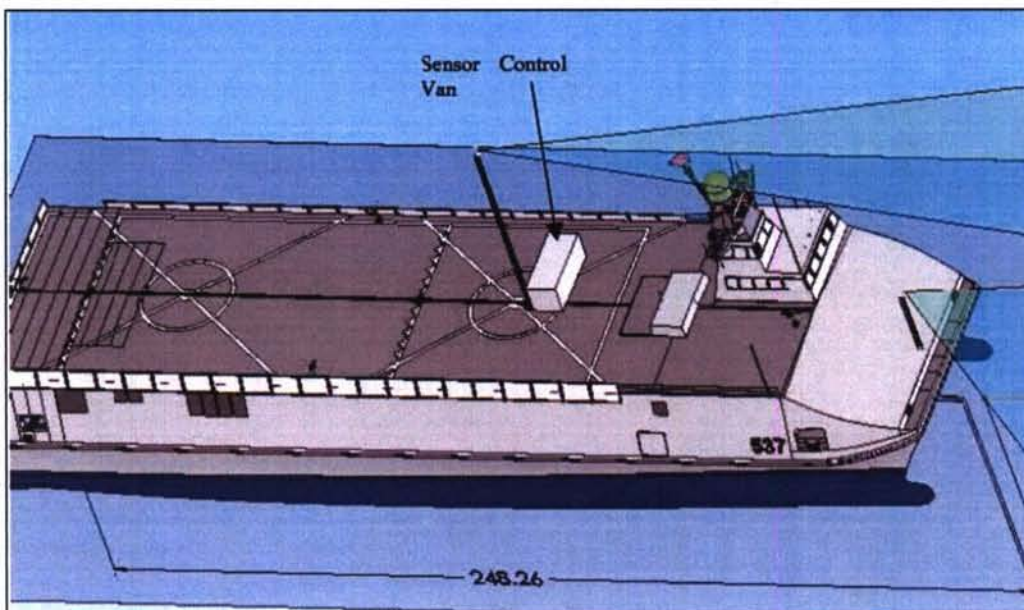
Figure 6. Drawing of the *Sea Fighter* showing locations of the forward LIDAR tower, the
x-band tower, and sensor control van.
The x-band tower is directly aft of the equipment van, approximately 17 ft aft of the
elevator. Units in the diagram are in feet.
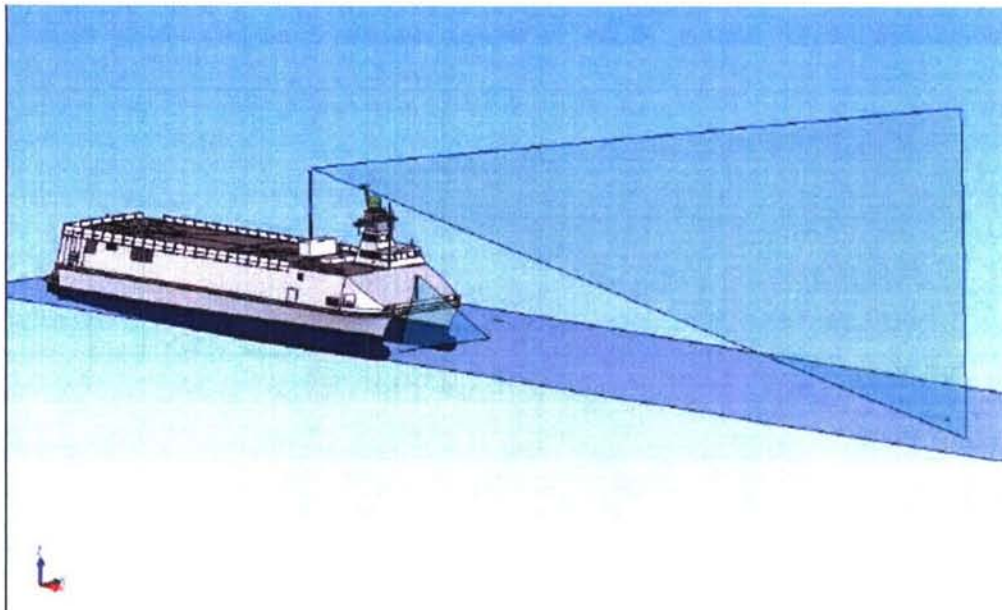
Figure 7. View of the forward LIDAR tower (with the LMS-Q140s scan swath) and the
x-band tower (with the WaMoS IIs scan beam).
Not shown is the vertical scanning LIDAR swath.
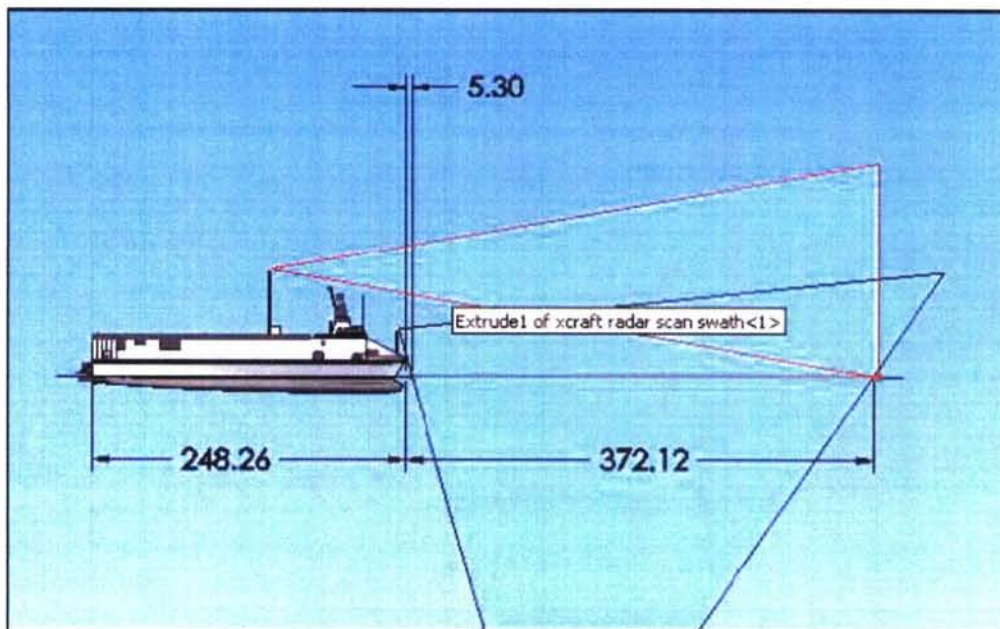
Figure 8. Side view of the *Sea Fighter* and instrumentation towers.
This figure shows the length of the ship; distance from bow to the LMS-Q240 LIDARs
swath (5.30 ft); and distance from bow to the x-band field-of-view (372.12 ft). All units
in diagram are in feet.
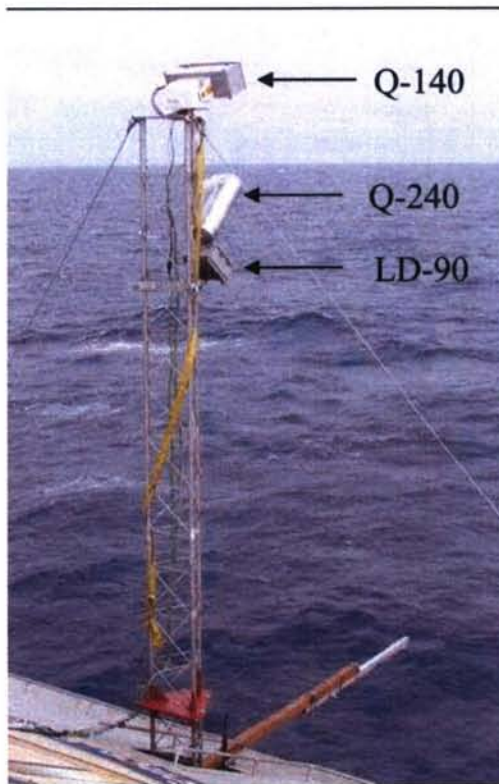
Figure 9. Photo of LIDAR tower on the *Sea Fighter*.

X-Band Wave Monitoring System (WaMoS)

The X-Band Wave Monitoring System (WaMoS II) uses the unfiltered output from a marine radar to determine wave and surface current parameters in near real-time. The system is composed of fast rpm Furono x-band marine radar (FAR2117BB, 6.5 ft antenna) whose output is digitized and sampled by a supplementary data acquisition system. This system processed data to provide significant wave height, mean period, peak period, mean wave direction, peak direction, peak wave length, 2D wave number spectrum, 2D frequency direction spectrum, 1st and 2nd peak period of the swell and wind sea, surface current velocity, and surface current direction. Raw image data generated by the x-band radar was continuously recorded to allow the development of wave retrieval algorithms to allow the tracking of individual surface waves. It was operated from a tower located on the maindeck of the *Sea Fighter* and resolved ocean waves located 330 ft to 6500 ft from the vessel. The tower height and its location were chosen to provide a complete 360 degree field of view to allow observation of both head and following seas. The x-band radar tower is 50 ft in length and is comprised of standardized 55G radio mast sections. The tower was hard mounted to the sensor control van that was secured to the flight deck of the *Sea Fighter*, just aft of the elevator as shown in Figure 6. The tower was guyed with steel cables to existing tie-down points located on the flight deck. The radar rotated 360 degrees at 42 rpm. Its beam was 20 degrees wide in the vertical, and 1.85 degrees wide in the horizontal. To ensure that the radar field-of-view was not

obstructed by any parts of the ship in all directions, the x-band tower stood 60 ft high and approximately 90 ft above the water surface so that it did not get returns from the existing superstructure onboard *Sea Fighter*. When looking forward, it viewed the sea surface approximately 372 ft forward of the ship's bow. The supporting electronics and computing resources for the x-band wave measurement system resided within the sensor control van directly beneath the tower. Figure 10 shows the location of the WaMoS-II and LIDAR towers onboard the *Sea Fighter*. Figure 11 is a photograph of the tower aboard the *Sea Fighter* during the test. The WaMoS data were not collected and analyzed by NSWCCD and will not be discussed in this report.
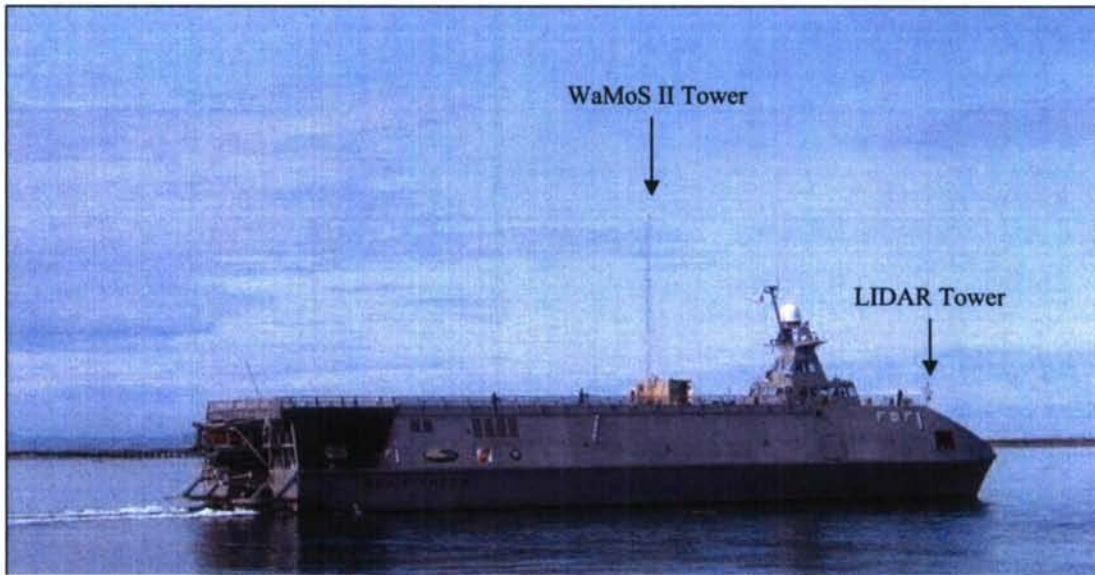
Figure 10. LIDAR and WaMoS (x-band radar) tower locations.

Figure 11. Photograph of x-band radar tower during testing.

Stereo-optic Measurement of the Sea Surface

The overall Stero-optic (S-O) system is schematically shown in Figure 12. A schematic of the camera-data acquisition-storage system is shown in Figure 13. The data acquisition system was tied into the available shipboard GPS time and position data stream to provide for synchronization of independent measurements and information for subsequent analysis. A three-camera system was used to provide two different S-O angles as well as a degree of redundancy. The camera/lens system was positioned to provide wave height measurements over a region nominally as wide as the ship and to cover distances forward of the bow ranging from 60 ft to as far as the wave fronts can be discerned. A schematic of the camera field-of-view is shown in Figure 14. Figure 15 provides details of the field-of-view geometry. The cameras were mounted on the forward deck, attached to the railing as shown in Figure 16. The cameras were mounted in housings, shown in Figure 17. The spacing of the cameras was determined by a trade-off between the need for accuracy of three-dimensional (3D) position determination requiring large spacing and the need to be able to identify specific discrete points in the field-of-view of each camera pair, requiring small camera separation. The highly accurate cameras acquired allow for 3D accuracy at relatively small separations.

Figure 12. Schematic of the Stereo-Optic Wave Measurement System.

Figure 13. Schematic of the Image/Data Acquisition System.

Figure 14. Schematic of stereo-optic system camera field of view.

Image Acquisition

The overall image acquisition system is shown in Figure 13. Three separate, but time synchronized image acquisition systems were used. Each system is composed of camera housing, a fiber optic cable, and a data acquisition c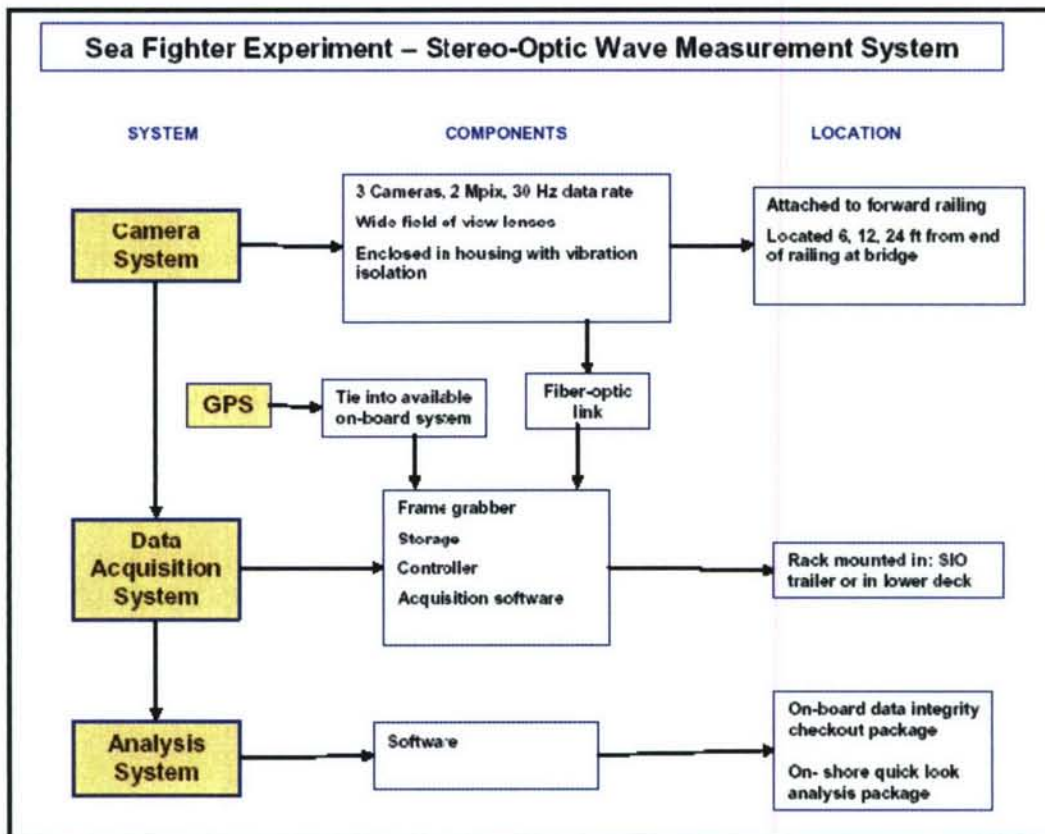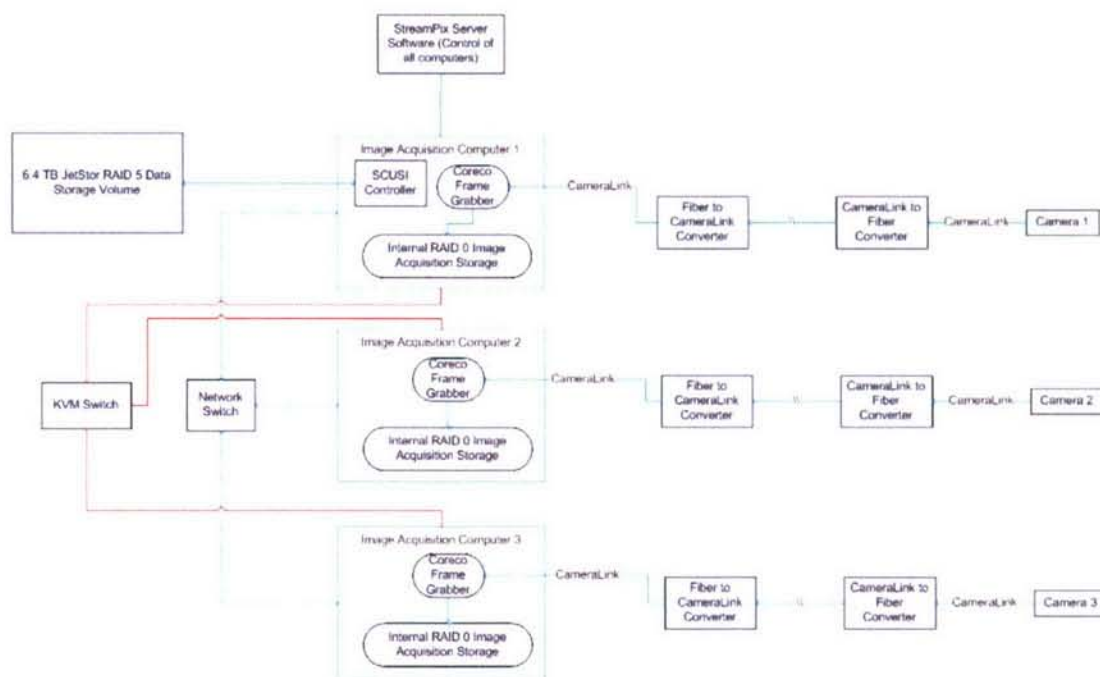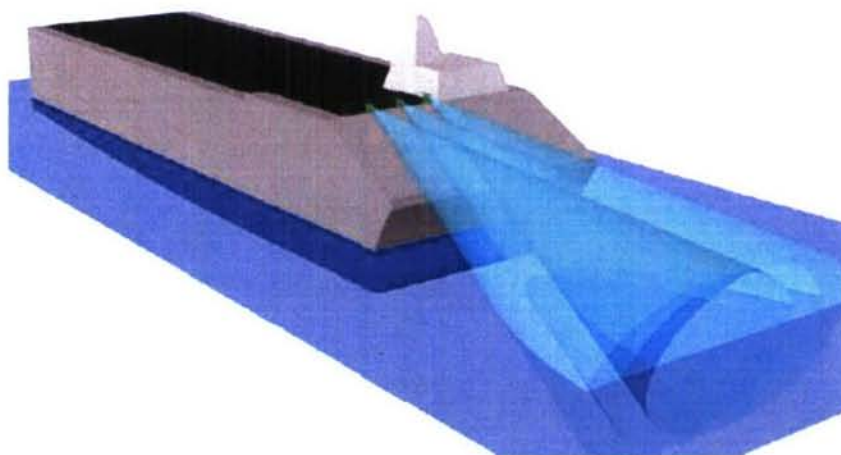omputer. The camera housing accommodates a two mega pixel camera, a power supply, and a fiber optic converter. Fiber optic cabling connects the camera housing to the data acquisition computer. The nominal distances between each camera, from left to right is 6 ft and 12 ft (see Figure 16). The end cameras comprised the primary image acquisition system. The middle camera was included as a backup system and a supplemental source of data. The cameras within the camera housing were aligned so that the baseline between the three cameras was collinear. The cameras also had a depression angle of 17 degrees so the field-of-view just encompassed the bow of the ship.

The image acquisition computers were located in the Mission Bay. Fiber optic cables linked the cameras through a plate that allowed cables to go from the Flight Deck to the Mission Bay. The computers were rack mounted in 2-12U SKB shock absorbing rack mount containers. Rack mounted equipment also included a 6.4 TB RAID Storage and an uninterruptible power supply (UPS) for power protection and stability. The power for the cameras and fiber link converters was run from the UPS to the camera housings. In total there were three cameras acquiring data and each camera had a dedicated computer with a Coreco X64-CL-iPro PCI-X framegrabber to acquire the images. Each computer also had an internal 1.2 TB RAID array for fast data acquisition. The RAID array consisted of 4-300GB hard drives in a RAID 0 (striped) configuration for maximum data transfer. StreamPix, a software package developed by Norpix, was used to drive the image acquisition process. Data were offloaded from the internal RAID drive to the 6.4 TB RAID storage drives at regular intervals after which the internal RAID drives were erased. One computer acted as a server controlling the acquisition process of all three computers. A National Instruments NI6601 timing board was used to trigger all three framegrabbers simultaneously. This insured that all images were acquired from the cameras at the exact same time. In order to maintain uniformity of the time stamp with the rest of the data taken during the test, GPS was synched to the computer's clock.
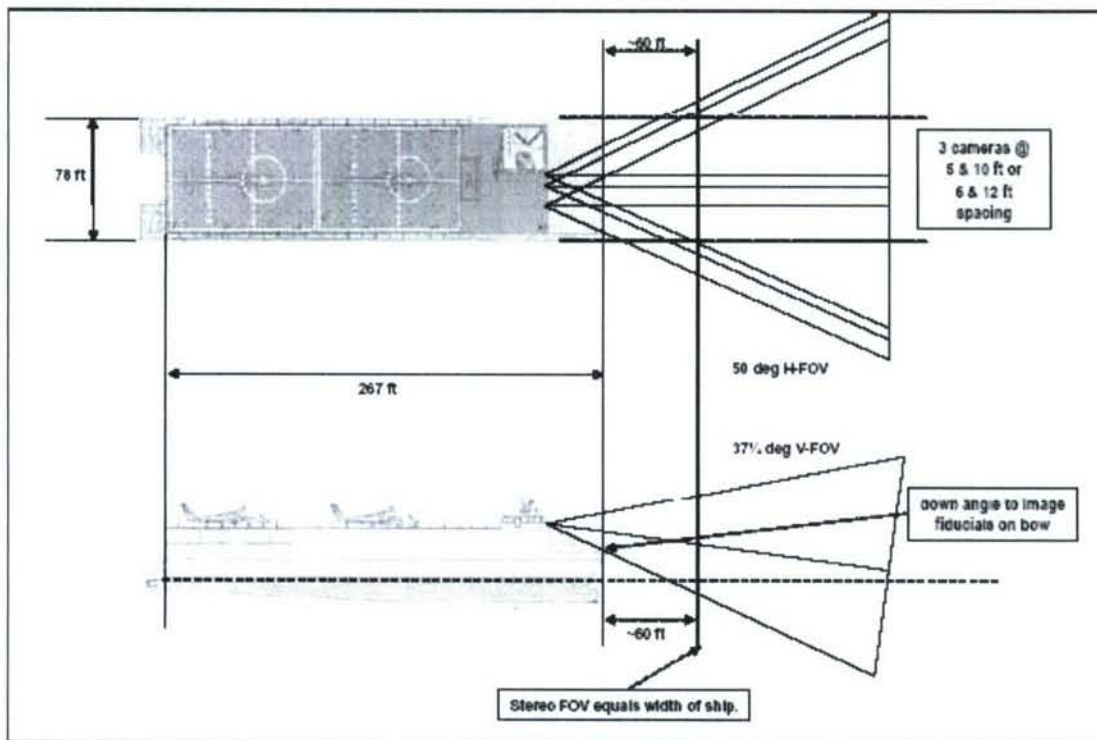
Figure 15. *Sea Fighter* Imaging Geometry.
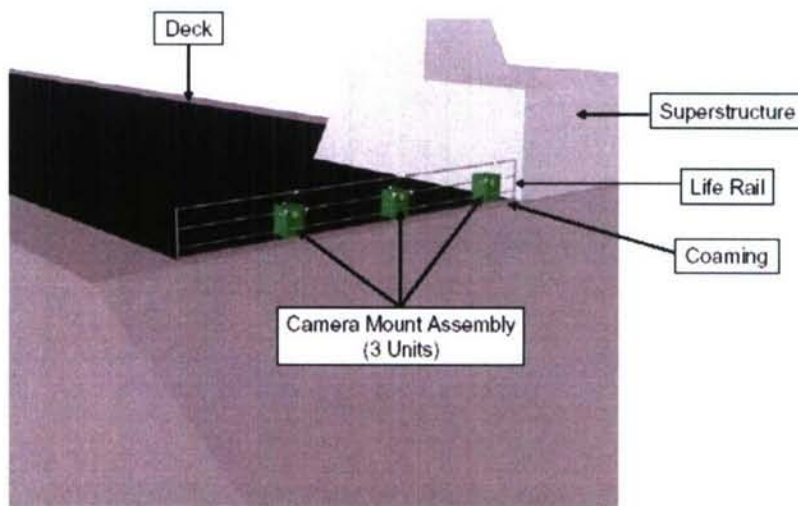
Figure 16. Camera deck arrangement.
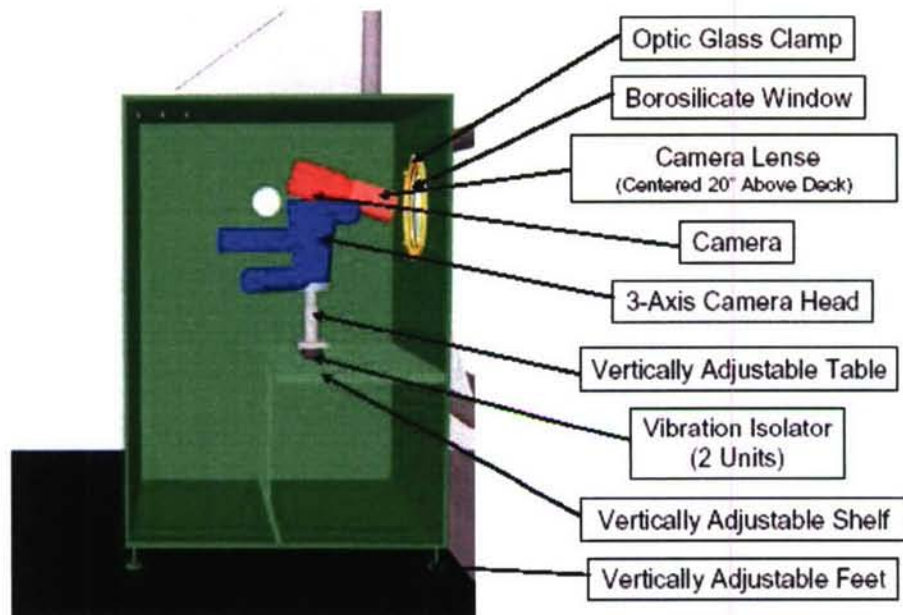
Figure 17. Camera mount arrangement.

Ship Motion Measurement

Vessel motion measurements were time-synchronized with the LIDAR and x-band measurements to measure vessel motion induced signals within the wave measurements. In addition, a combined GPS and inertial package as well as three Litton LN200s were on board to record ships motions. Only the data collected by the GPS/Inertial package and LN200's will be discussed in this report.

Combined GPS and Inertial Motion Package

The combined motion package was installed near the vessel centerline and slightly aft of the second forward most watertight bulkhead as shown in Figure 18. The motion package consisted of a gyro enhanced orientation sensor (3DM-GX1), a SUPERSTAR II GPS, and a Persistor CF2 CPU. The 3DM-GX1 sensor consists of three angular rate gyros, three orthogonal DC accelerometers, three orthogonal magnetometers, and a multiplexer. The gyros track dynamic orientation while the accelerometers and magnetometers track static orientation. The 3DM-GX1 combines the static and dynamic responses in real time and records 20 samples per second. The SUPERSTAR II GPS provides position, velocity, and time data once every second. The CF2 runs on battery power and combines and stores the collected data on a flash disk. A complete list of the data recorded by this package is provided in Table 3.

LN200 Package

Three Litton LN200s were installed aboard the *Sea Fighter*. Each LN200 is an inertial measurement unit consisting of three fiber optic gyros and three linear accelerometers. Table 3 provides a complete list of the data collected by these packages. An LN200 was mounted in the bow of each hull (port and starboard) along the hull's centerline and the third package was mounted in the Mission Bay starboard of the vessel

16

centerline as shown in Figure 18. This configuration allowed for the motion of each hull and the overall ship to be examined and compared. The three LN200 inertial motion units provided linear and angular accelerations, angular rates, roll, pitch, and heading data all taken at a sampling rate of 200 Hz.
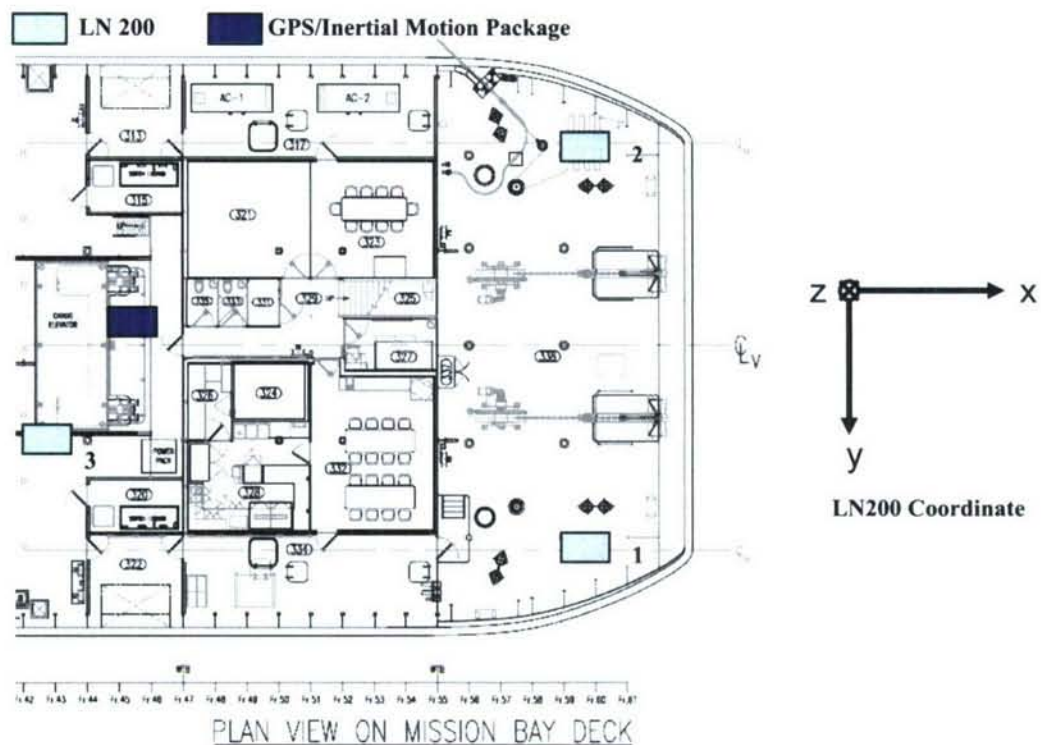
Figure 18. Locations of ship motion packages.

Table 3. Summary of data collected by LN200 and GPS/Inertial motion package.

	LN200	GPS/Inertial Package
Heading	X	
Pitch	X	X
Roll	X	X
Yaw	X	X
X Linear Acceleration	X	X
Y Linear Acceleration	X	X
Z Linear Acceleration	X	X
X Angular Acceleration	X	
Y Angular Acceleration	X	
Z Angular Acceleration	X	
X Angular Rate	X	X
Y Angular Rate	X	X
Z Angular Rate	X	X
Latitude		X
Longitude		X
Altitude		X
Ground Speed		X
Track Angle		X
N. Velocity		X
E. Velocity		X
V. (Total) Velocity		X
Date		X
Time		X

RESULTS

The overall test plan objective was to measure the wave elevation and ship motions while undergoing high speed slamming events. Data were collected continuously throughout the four day trial. Four slam events were identified and analyzed and are listed in Table 4. A slam event was determined by the encounter of a wave that was large enough to make impact with the wet deck (refer to yellow arrow in Figure 19). Three of the events occurred on the same day while cruising at speeds in the range of 15 to 20 knots, while the fourth event occurred the day before while traveling at a higher speed of 30 knots. For each event the wave field was characterized using the ultrasonic sensors and ship motions were analyzed.

Table 5 summarizes the sea state data collected by three independent instruments; a TSK Shipborn Wave Height Meter, a Neptune buoy, and a NOAA buoy. Additional details about each instrument can be found in Appendix A. The rows highlighted in yellow provide sea state data for the slam events listed in Table 4. The wave heights seen by all four events were between 8.5 and 8.9 ft. Approximately 6 second wave periods were seen on the 20th while 10 second periods were seen on the 19th.

Table 4. Slam Events Summary.

Slam Event	Date	Time (GMT)	Speed (knt)
1	19-Apr-06	2:33	30.0
2	20-Apr-06	19:30	19.8
3	20-Apr-06	21:36	16.4
4	20-Apr-06	22:08	15.8

Table 5. Summary of sea state data from TSK, Neptune Buoy, and NOAA Buoy.

Date, GMT	Time, GMT	TSK Run No.	Waveheight		Period		Dir, deg-M	Buoy No.
			Hs, ft	Hs, m	To, sec	Ts, sec		
TSK								
19-Apr-06	1915	124	6.5	2.0	6.8	-	-	TSK
19-Apr-06	2155	130	6.3	1.9	9.1	-	-	TSK
20-Apr-06	130	140	6.3	1.9	9.1	7.4	-	TSK
20-Apr-06	1825	143	8.5	2.6	5.9	16.4	-	TSK
20-Apr-06	2320	157	8.9	2.7	6.3	16.4	-	TSK
Neptune Buoy								
19-Apr-06	1500	-	4.9	1.5.	11.0	6.0	NNW	A24
20-Apr-06	1627	-	6.4	2.0	7.4	-	321	A24
20-Apr-06	1655	-	6.9	2.1	6.9	-	6	A24
NOAA Buoy								
19-Apr-06	300	-	8.5	2.6	10.0	-	WSW	46087*
19-Apr-06	427	-	8.2	2.5	9.1	7.7	WSW	46087
19-Apr-06	455	-	7.9	2.4	8.3	-	WSW	46087
20-Apr-06	1500	-	7.6	2.3	7.1	-	332	46028**
20-Apr-06	1600	-	7.7	2.3	6.7	-	324	46028
20-Apr-06	2300	-	7.6	2.3	16.1	7.1	308	46028

* NOAA bouy 46087 located at 48.49N, 124.73W - Neah Bay (Entrance to Juan de Fuca Strait)

**NOAA buoy located at 35.75N, 121.89W - 30 to 40 nm NE maneuvering hexagon (see Figure 3)
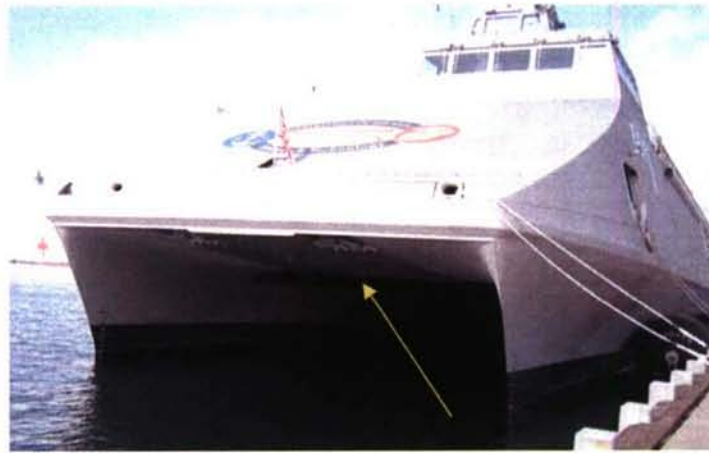
19

Figure 19. Schematic showing the bottom of the hull that required impact to define a slam event.

Wave Field Characterization

The data collected by the ultrasonic sensors was used to characterize the wave field seen by the ship before, during, and after each slam event. Due to the rough test environment (sea state 4) the data collected by the ultrasonic sensors had more signal losses than typically seen when using the instruments for experiments in the tow basin. Therefore, the raw data first needed to be filtered and the losses corrected. Signal losses were identified based on the slope between adjacent points. If the absolute value of the slope between two points was greater than a given threshold, 10 ft/msec, then those data points were flagged as part of a signal loss. The threshold was chosen based on the sea state information and instrument capabilities. Data from the ultrasonics were collected at 10 Hz, therefore, in sea state 4 conditions it is highly unlikely that a wave steepness of that magnitude could be achieved in only 0.1 seconds; that would require the wave height to change by 10 ft in only 0.1 seconds.

After a data point was flagged as part of a signal dropout its value was reset to zero. The dropouts, now zero values, were then filled in by linearly interpolating between the two nearest non-zero values (the last recorded value before the loss and the first point once reconnected). Figure 20 and Figure 21 show an example of the raw data (with dropouts) and the corrected data for the port bowline sensor for Slam Event 2. The dropouts in the raw data can be recognized as the steep vertical blue lines. The gap in the data shortly after 19:29 GMT, denoted by the flat red line is different than an ultrasonic dropout. It is caused by a loss of the time feed into the data acquisition program and is a loss of data that can not be replaced; therefore these gaps remain in the data sets while dropouts are corrected. As seen by Figure 20 and Figure 21 it was impossible to eliminate every dropout, however, the majority of dropouts were identified and corrected, producing a more complete set of data to use in analysis.
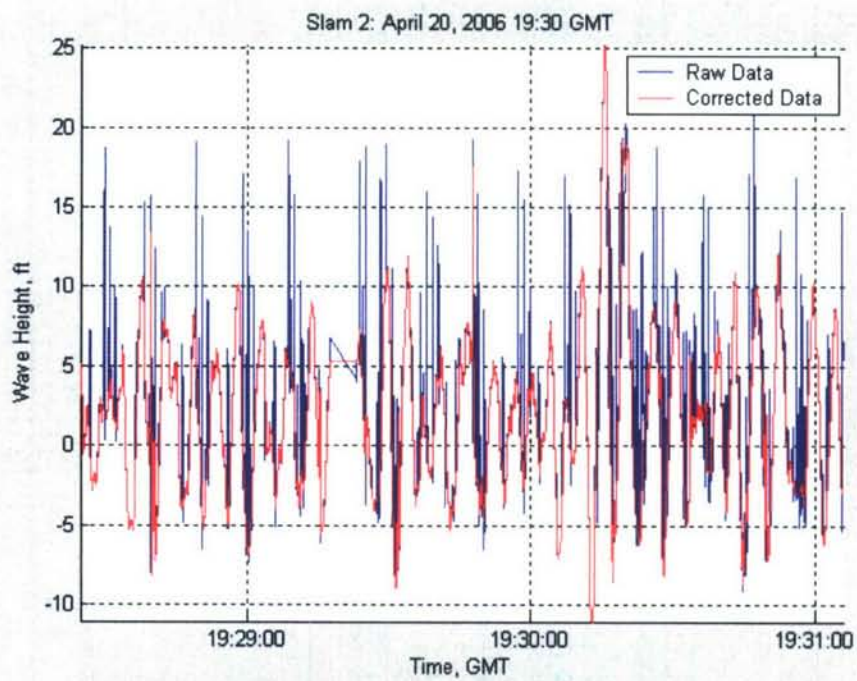
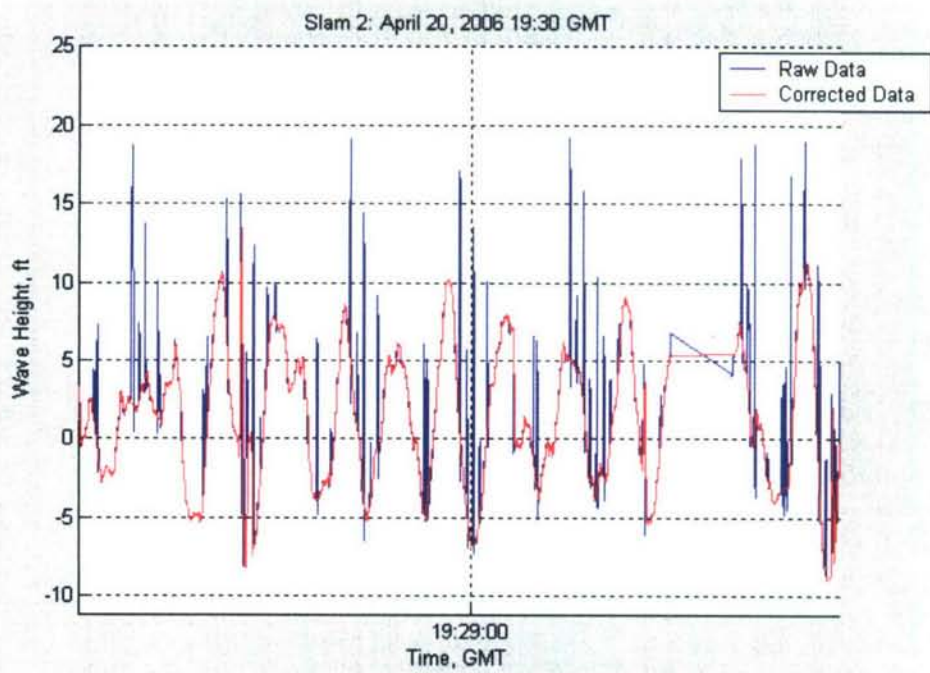Figure 20. Example of raw and corrected ultrasonic data.

Figure 21. A zoomed in view of Figure 20.

21

In addition to correcting the data for signal losses the data also had to be corrected for ship motions. Motion data from LN200 package 3 was used because it was located closest to the ship CG. Given the distance of the instrument from the CG the height in the ultrasonic readings due to ship motions was determined using equations 1 and 2. This height, z_{pitch} and z_{roll}, was then removed from the ultrasonic readings. The derivation of these equations is illustrated in Figure 22.

$$z_{pitch} = d_{cg} \cdot \sin \theta \tag{1}$$

$$z_{roll} = d_{cg} \cdot \sin \phi \tag{2}$$

Where: d_{cg} = longitudinal or transverse distance to ship CG

θ = pitch angle from LN200 3
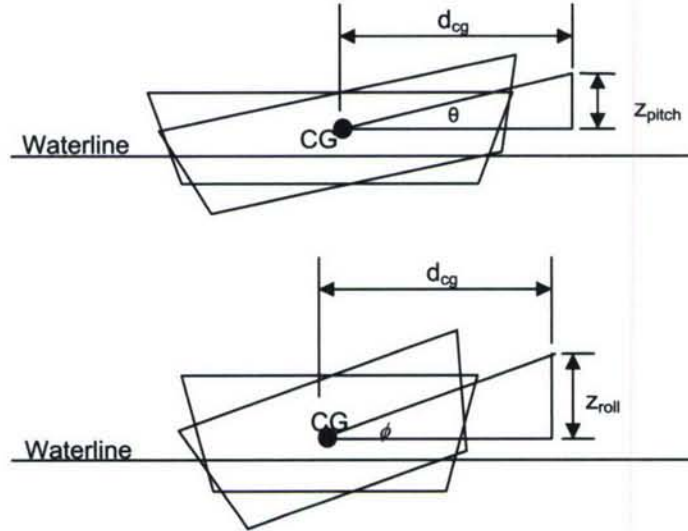
ϕ = roll angle from LN200 3

Figure 22. Diagram illustrating derivation of Equations 1 and 2.

Once the raw data were corrected the wave field was able to be determined. Figure 23 shows a portion of the corrected data for all the bow ultrasonics for Slam Event 2. In total, there were nine bow ultrasonics, (refer to Figure 6 and Table 2 for details of the ultrasonic locations) however, the starboard aft anchor ultrasonic is not included in the data set because it was damaged earlier in the test. The purple trendline is data collected by the center ultrasonic and Figure 23 shows that it still has a significant number of dropouts even after the data was processed to help eliminate the dropouts created by a signal loss. The center ultrasonic, as well as the port and starboard ultrasonics, was mounted on a boom that projected out from the front of the ship. This allowed the spread angle of the ultrasonics to not be obstructed by any part of the ship. While in rough seas, especially during a slam event, the boom itself had its own motion making it difficult to keep a continuous signal of data. It is assumed that the increase in the number of dropouts seen by these ultrasonics is due to this mounting configuration.

22

Based on the data shown in Figure 23 it was determined that each ultrasonic, regardless of its location along the bow of the ship saw the same wave field. Therefore, it was determined that the data collected by the center, port, and starboard ultrasonics could be omitted from further analysis without altering the final wave field characterization.
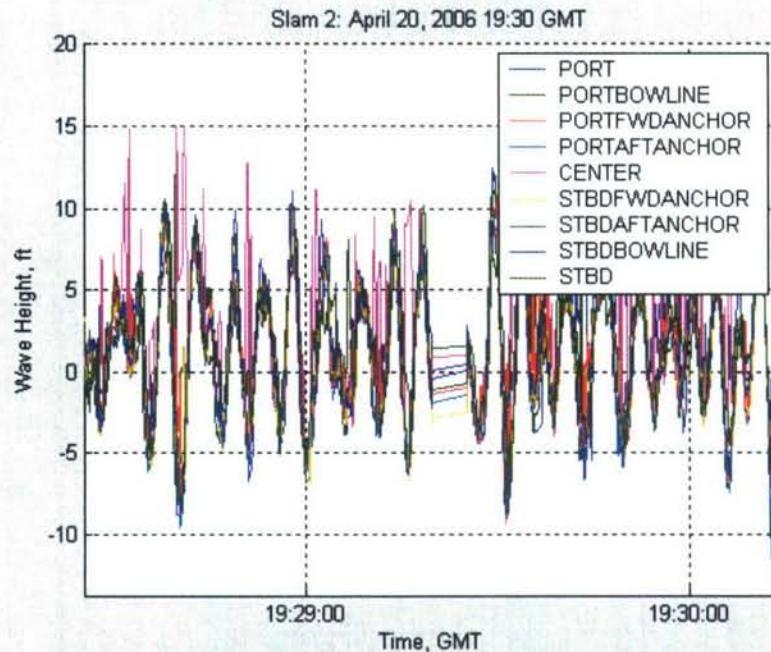

Figure 23. Plot of all bow ultrasonics for Slam Event 2.

Once the port, starboard, and center ultrasonics were omitted from the analysis the four sensors mounted in the anchor wells were compared to one another to determine an overall anchor well wave profile and the same analysis was applied to the port and starboard bowline sensors. Figure 24 shows the comparison of the port and starboard bowline sensors. The blue and red trendlines represent the corrected data for the port and starboard bowline sensors respectively. The figure shows that the data collected by both sensors was very similar, and therefore, an average between the two was calculated and used in determining the overall wave field during this event.

The same approach was used in analyzing the data from the anchor well sensors. Figure 25 shows the data from the three functioning anchor well ultrasonics. All three ultrasonics show similar wave fields, however, the port forward anchor ultrasonic still has various dropouts after the slam event that were unable to be corrected. Therefore, this ultrasonic was omitted and the port aft and starboard forward ultrasonics were averaged to determine the average anchor well wave profile. The anchor well average and bowline average were then averaged to determine the overall wave field seen by the vessel before, during, and after the slam event. Figure 26 shows the anchor well and bowline averages and the final average between the two. Figure 27 shows the final wave profile for Slam Event 2.
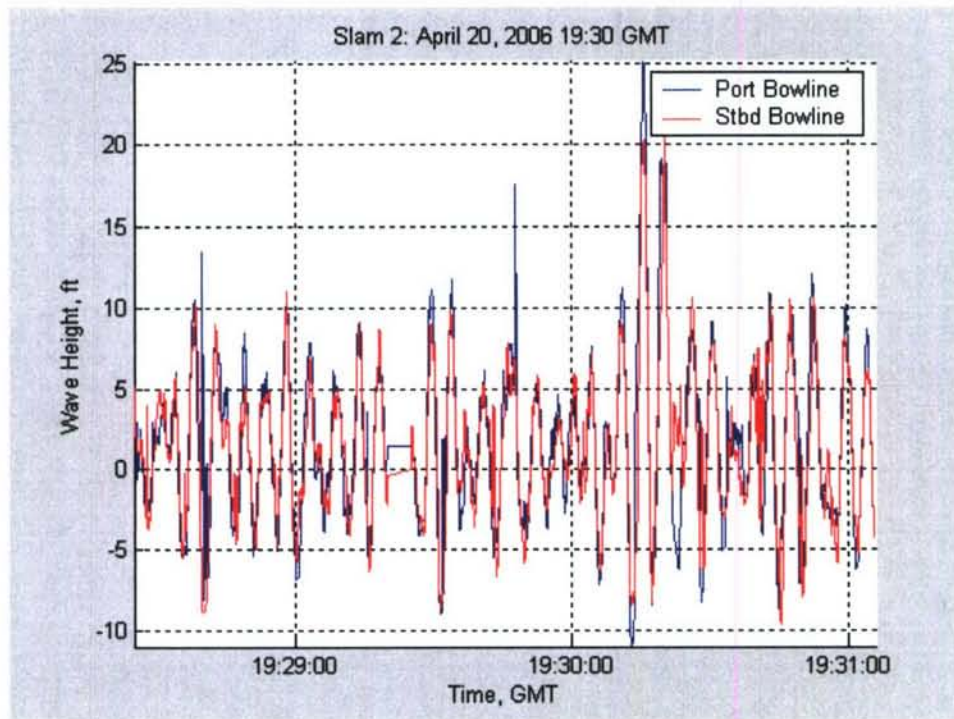
23

Figure 24. Slam Event 2: Bowline Ultrasonics.
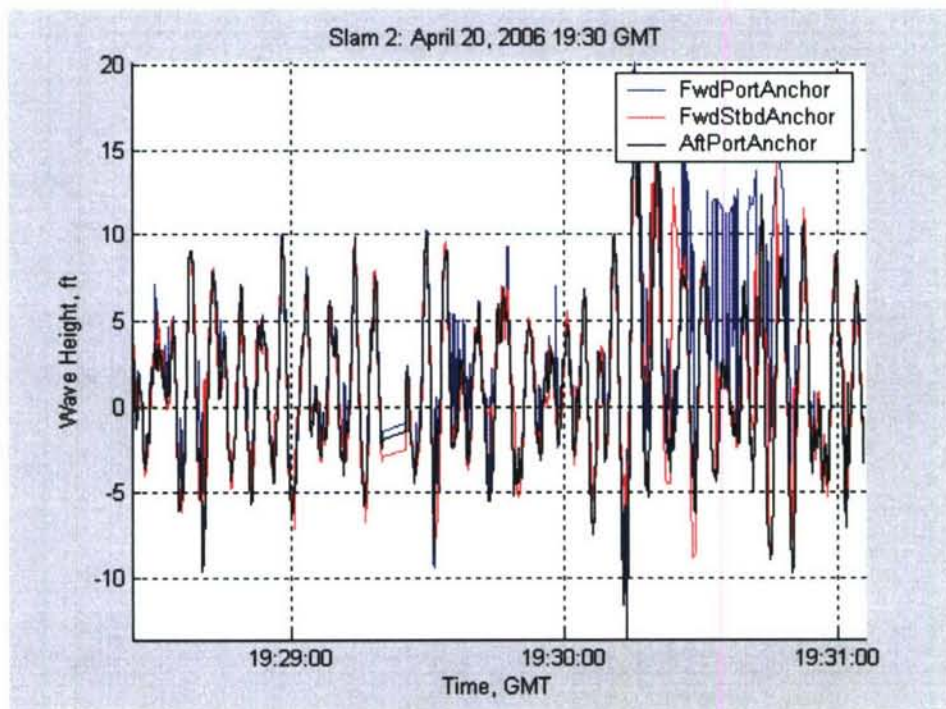

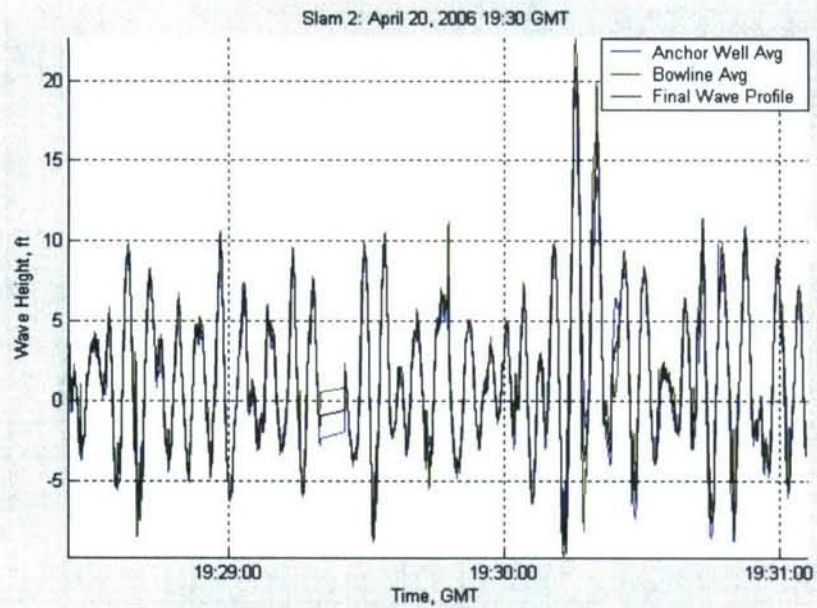Figure 25. Slam Event 2: Anchor Well Ultrasonics.

24

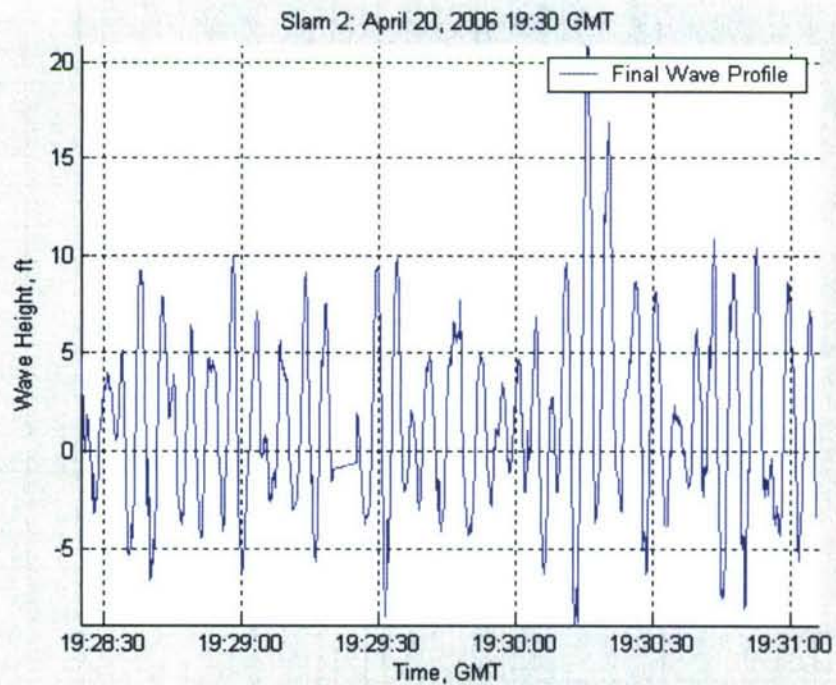Figure 26. Slam Event 2: Anchor well average, bowline average, final wave profile.

Figure 27. Slam Event 2: Final Wave Field Profile.

This approach of comparing sensors to one another and determining an average profile for a given bow location was then used in determining the overall average wave field for each slam event. The final wave field for each slam event is shown in Figure C1-Figure C4 in Appendix C.

Ship Motion Measurement

Ship motions were measured using two separate motion packages; a set of three Litton LN200s and a combination GPS and inertial motion package. Figure 28 shows a comparison between the three LN200s and the motion package for ship pitch during Slam Event 4. All four instruments show the same trend in the data. The data from LN200 1 and LN200 2 practically lie on top of one another and only have a small phase shift from LN200 3 which has a short lag time behind the motion package. This small variation in signal is due to the location of the instruments on board *Sea Fighter* (refer to Figure 18). LN200 1 and 2 were both roughly the same distance forward of the center of gravity and equal distances longitudinally off the vessel centerline, making the data collected by each very similar as expected. LN200 3 and the motion package were located aft of LN200 1 and 2, closer to the vessel CG; and this is reflected in their data. It is important to note that there is limited control in a full scale in situ experiment. Therefore, it is also likely that there is some roll contamination in the pitch readings and vice versa due to an inability to mount the instruments completely level which may also be a contributing factor in the variations seen in the ship motion instruments. This comparison of the motion packages was used to further validate the data collected by each instrument showing that each was functioning properly during the trial.
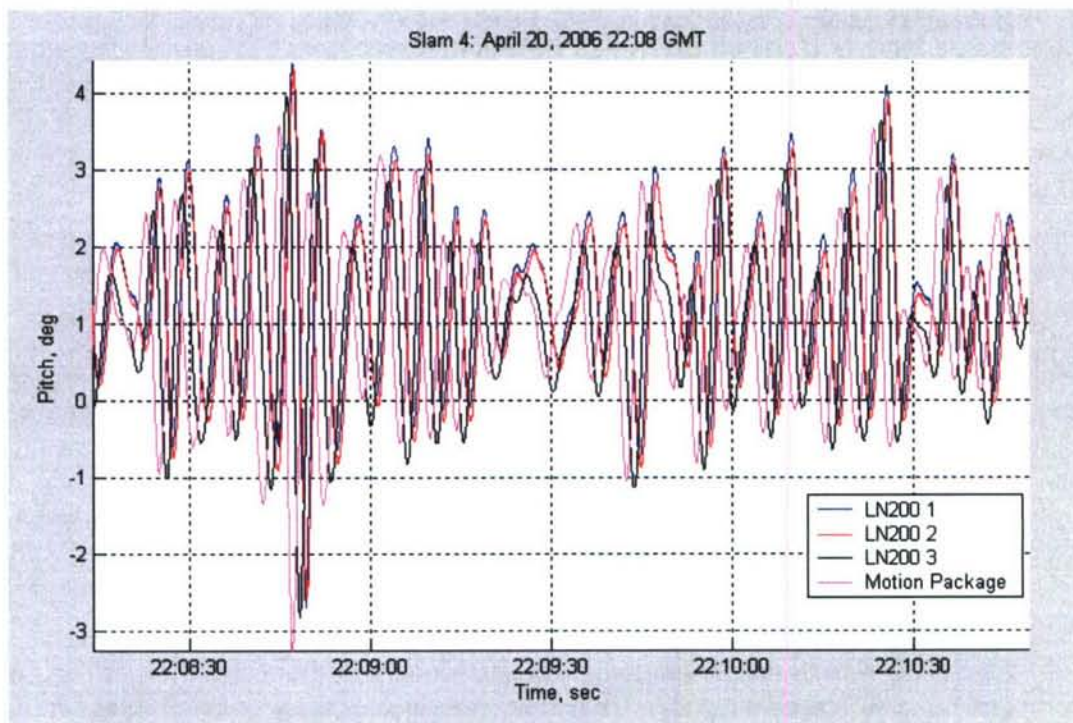

Figure 28. Pitch comparison between ship motion packages.

Some conclusions can be drawn from the comparison among the LN200s. The instruments were specifically chosen to be placed one in each of the side hulls and one near the centerline of the vessel to examine ship bending during high impacts events. The consistency throughout the slam event of the data in Figure 28 shows that no significant bending has occurred. However, due to the possibility of roll contamination and without additional instruments such as strain gages mounted in each hull, it is difficult to completely eliminate the possibility of some bending due to a slam event. Additional structural data and analysis for *Sea Fighter* will be reported by NSWCCD, Code 60.

Combined Results

To completely characterize a slam event it was necessary to look at the ship motions, wave field data, and the video from the underway cameras together and draw conclusions. Specifically slam events at the bow were analyzed, therefore LN200 1 was used for the analysis of the ship motions because it was located closest to the bow of the ship (LN200 2 could have been used as well since the only difference between its location and the location of LN200 1 is that it was mounted port of the vessel centerline). Each slam can be identified by a large wave that has a significant impact on the ship's motions. A significant impact is defined as motions that are outside of an average envelope of motions seen for a given time period.

Slam Event 1

Figure 29 provides wave height, pitch, and vertical linear acceleration plots for Slam Event 1. There are two slams that occur over the given time period and both can be recognized by the spikes seen in the z linear acceleration plot. It is important to note that the y-axis in the z linear acceleration plot is actually a measure of the change in z linear acceleration in g-force. Therefore, 0 g's is the standard acceleration due to gravity and any value below or above it corresponds to additional acceleration of the ship. For example, when the graph spikes close to 1 g as in Figure 29 then the ship is experiencing 1 g of vertical acceleration in addition to its vertical acceleration due to gravity.

From Figure 29 it can be seen that the pitch of the ship varies from approximately 0 to 2 degrees and linear acceleration varies from ±0.2 g's. The wave heights start in a -10 to 0 ft envelope and then shifts up to a ±5 ft envelope. The slam occurs shortly after 2:33:30 GMT and can be identified on the graph by the sharp spike in z linear acceleration. It involves three consecutive increasing crests, all above the bounds of the 5 ft envelope. The first two crests cause a slam with the second crest producing the most violent slam, as seen by the large spike in vertical acceleration. In addition, during the trough before the second crest the bow of the ship rises out of the water and is suspended in the air just before the second crest slams into the bow. With the second crest the bow pitches down to the minimum pitch angle for this time period, -2 degrees, then quickly pitches up to 4 degrees (the maximum) and pitches down again to 1 degree with the final crest.

Figure 30 shows this sequence of events using the on-board bow center and starboard cameras respectively. The first row of snapshots show the first crest which causes a small slam, but it is not large enough for white water to be seen by the center

27

camera. The second row of photos shows the first trough that lifts the bow out of the water just before the second slam. The third row shows the second crest slamming into the bow, which is the most violent slam of the three crests. The intensity of the slam can be seen by the large amount of whitewater in the bow camera view in both the third and fourth row photos. The fourth row shows the following trough and the remnants of the previous slam can still be seen by the white water and spray that is still present in the bow center camera. The last row shows the last crest which is the largest crest in the wave height plot, but it does not produce a slam.
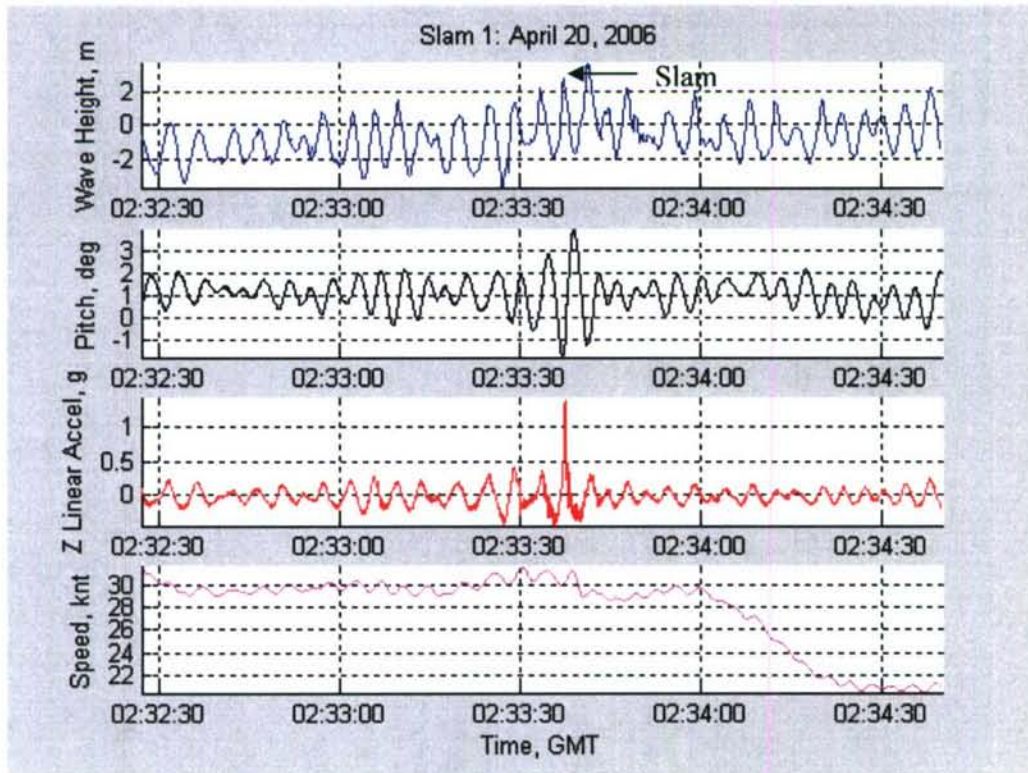

Figure 29. Slam Event 1: Wave Height, Pitch, Vertical Acceleration, and Speed plots.

1st crest: Small slam

1st trough: Bow lifts out of water

2nd crest: Slam

2nd trough: White water from previous slam

3rd crest: White water from previous slam

Figure 30. Slam Event 1: Snapshots of on-board cameras. The first row shows the small slam due to the first crest and the third row shows the second, more violent slam.

Slam Event 2

Figure 31 provides plots of the wave height, pitch, and z linear acceleration data for Slam Event 2. The spikes in all three graphs at approximately 19:30:15 GMT indicate the actual slam event. For this given time period the wave heights stay within a ±10 ft range except during the slam when the wave crests double in size. Similarly, pitch stays steady in a range of 0 to 2 degrees and then increases to a range of -2 to 4 degrees during the slam. Finally, the z linear acceleration fluctuates between ±0.2 g's and spikes to ±0.4 g's during the slam.

The event begins with a 5 ft wave trough which is followed by a 20 ft crest, a trough of 2 ft and another large crest over 15 ft. Both troughs cause the bow of the vessel to completely lift out of the water and both crests cause a slam impact with the bow. Figure 32 provides snapshots from three of the on-board cameras (starboard, center, starboard bowline respectively) showing the sequence of events of the slam as described. The first row of snapshots shows the ship encountering the first trough when the bow lifts completely out of the water. Row 2 shows the impact of the first crest and the small slam it causes. The third row shows the second trough and the bow again lifting out of the water. Finally, the fourth row of snapshots shows the larger slam caused by the impact of the second crest.
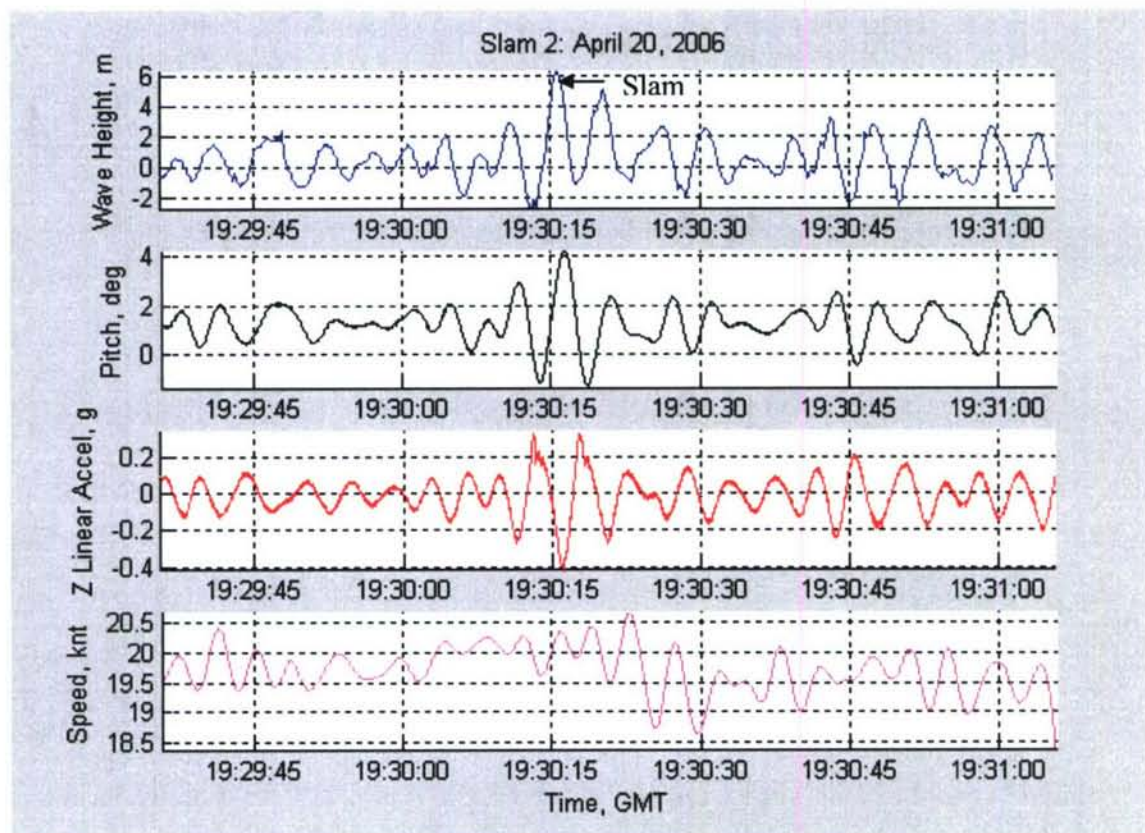

Figure 31. Slam Event 2: Wave Height, Pitch, and Vertical Acceleration, and Speed plots.
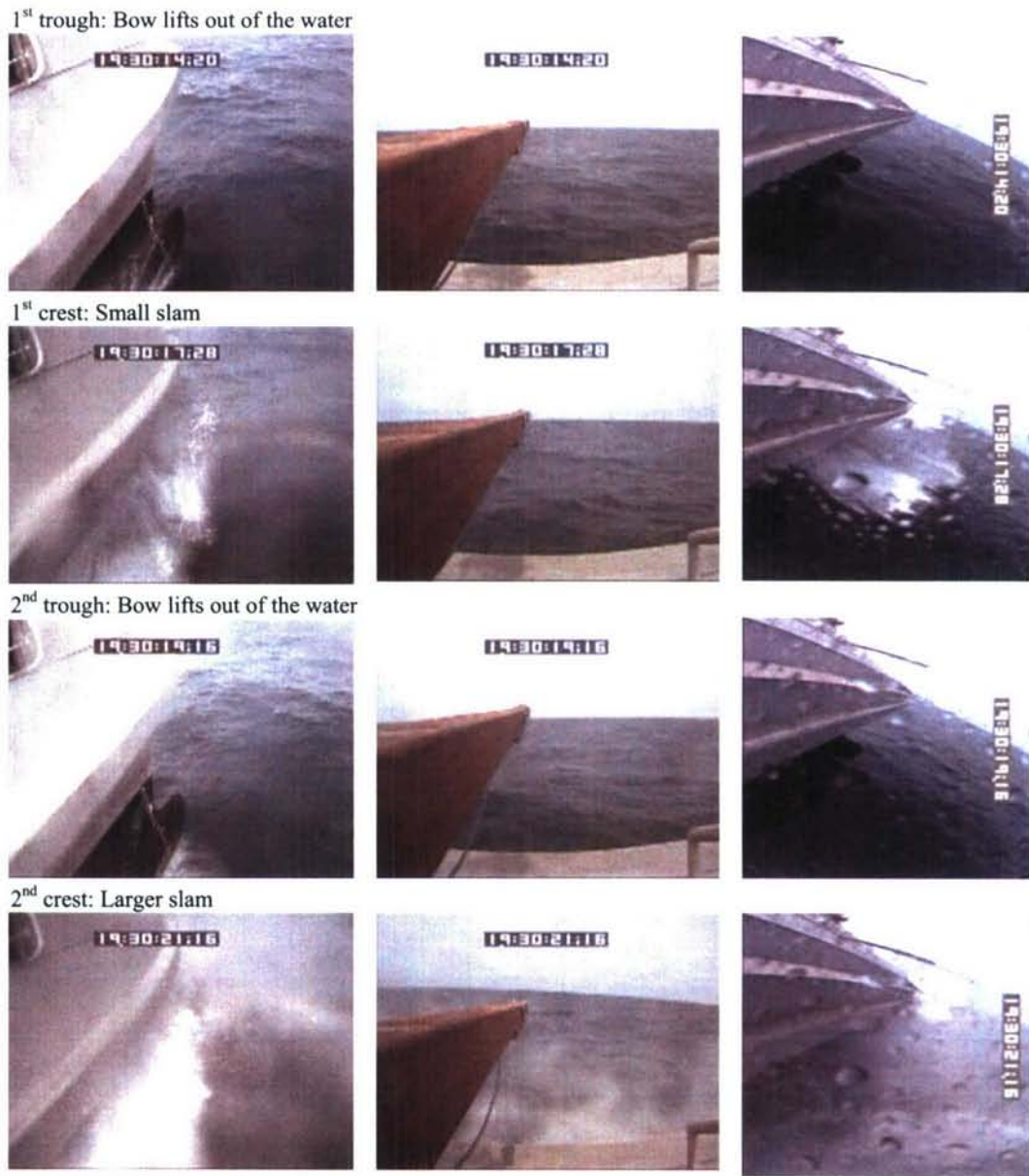
1st trough: Bow lifts out of the water

1st crest: Small slam

2nd trough: Bow lifts out of the water

2nd crest: Larger slam

Figure 32. Slam Event 2: Snapshots from on-board cameras.

Slam Event 3

Figure 33 provides wave height, pitch, and z linear acceleration plots for Slam Event 3. There are three separate slam events in the time span shown in the figure. There is one shortly after 21:38:00 GMT, labeled A on the graph and denoted by the largest spike in z linear acceleration seen. Slam B occurs at approximately 21:38:45 GMT and Slam C occurs towards the end of the plot near 21:39:30 GMT. On average the wave heights stay within an envelope of ±10 ft. When the wave heights are greater than ±10 ft then it is likely a slam occurs. Similarly, pitch stays within a range of 0 to 3 degrees

31

except during a slam where it oscillates from -2 to 4 degrees. In addition, the ship experiences a steady vertical acceleration of ±0.2 g's except for during a slam.

The most significant slam is Slam A which occurs at approximately 21:38:00 GMT. It begins with a large crest of almost 15 ft followed by a trough of about 8 ft and then a larger crest of over 20 ft followed by another almost 8 ft trough. The slam occurs as the ship encounters the second and larger crest which can be seen by the large spike in vertical acceleration up to 0.5 g's. Figure 34 shows snapshots of three of the onboard cameras during the slam event; the starboard, center, and starboard bowline cameras respectively. The first row in Figure 34 shows the first (15 ft) crest and the second row shows how the bow of the ship comes completely out of the water as it encounters the first 8 ft trough. Next, as seen in the third row and fourth rows, the 20 ft crest slams into the bow causing the large spike in vertical acceleration. The second 8 ft trough (fifth row) causes the bow to rise out of the water again; however the next crest is not large enough as seen by the sixth row of snapshots to cause additional slamming.
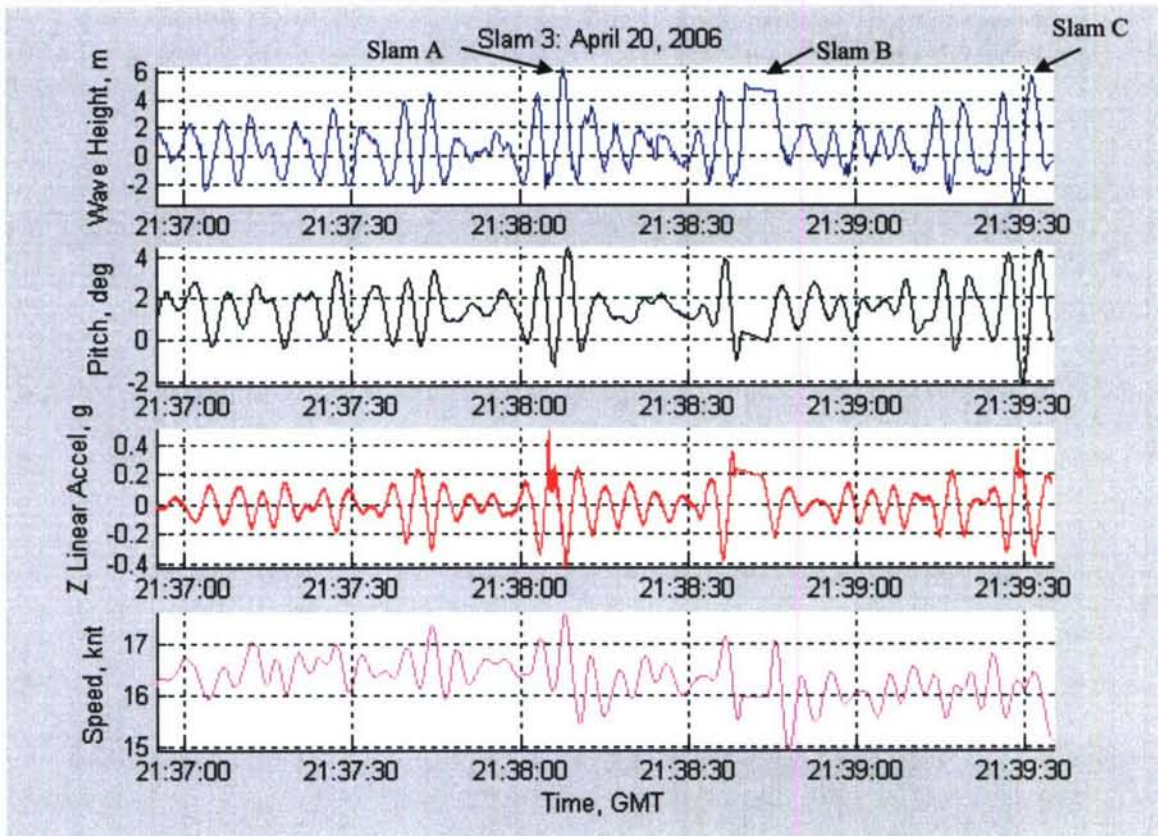

Figure 33. Slam Event 3: Wave Height, Pitch, Vertical Acceleration, and Speed plots.

1st crest

1st trough: Bow lifts out of the water

2nd crest: Slam

2nd crest: Slam

2nd trough: Bow lifts out of the water

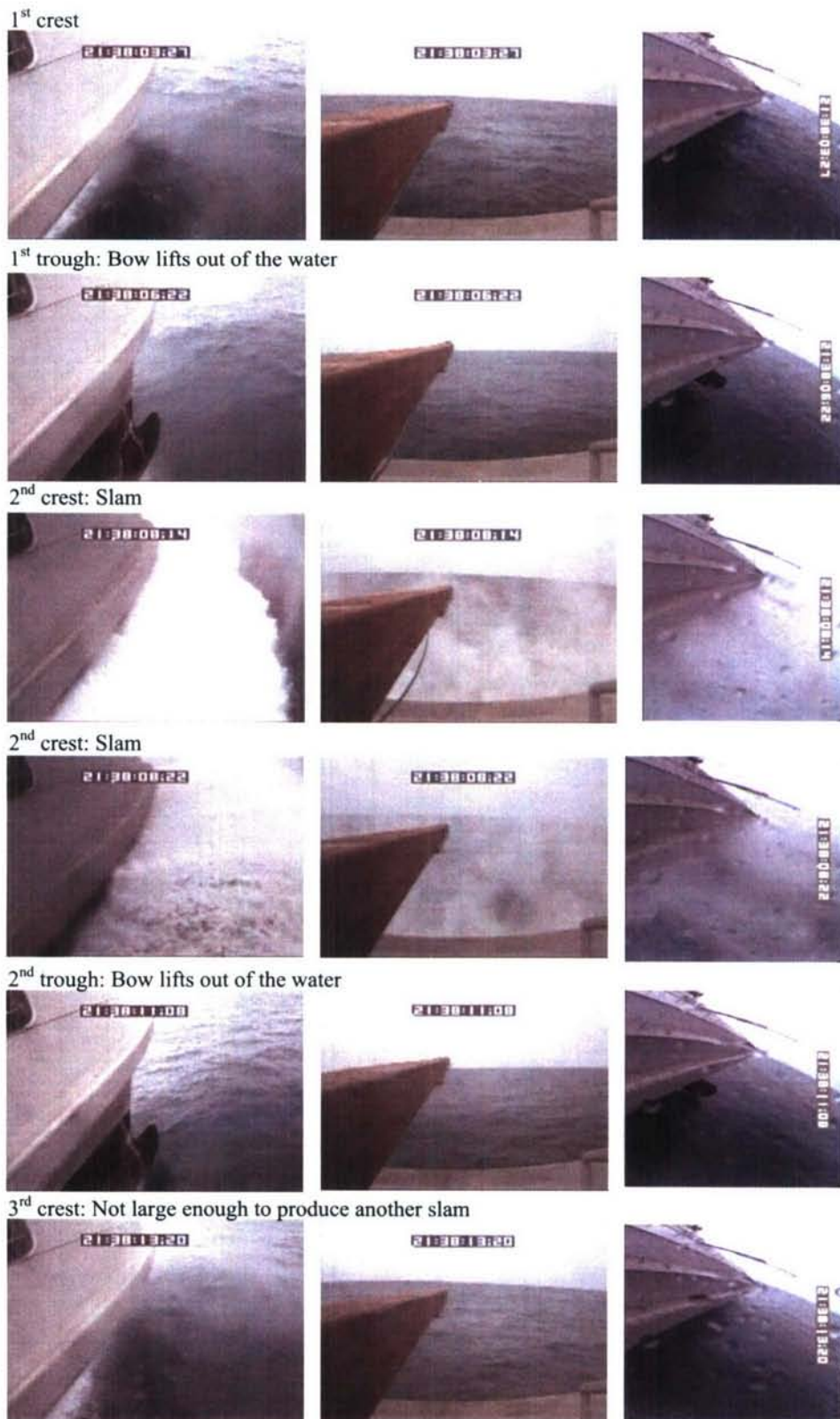3rd crest: Not large enough to produce another slam

Figure 34. Slam Event 3A: Snapshots from on-board cameras.

Slam B occurs about 45 seconds after the first. Again it begins with a larger than average wave crest of 15 ft followed by an 8 ft trough, and a second slightly larger crest. Unfortunately, at this point the data acquisition program lost its signal and data was briefly lost but the on board cameras were able to visually fill in this data gap. Figure 35 shows this sequence of events. The ship encounters the first crest which comes close to hitting the bottom of the wet deck but is not large enough to cause a slam. The following trough, like the first slam, causes the bow to lift out of the water and pitch up at almost 4 degrees and the second crest is large enough to slam into the bottom of the hull causing the bow to pitch down and an increase in vertical acceleration to almost 0.4 g's.
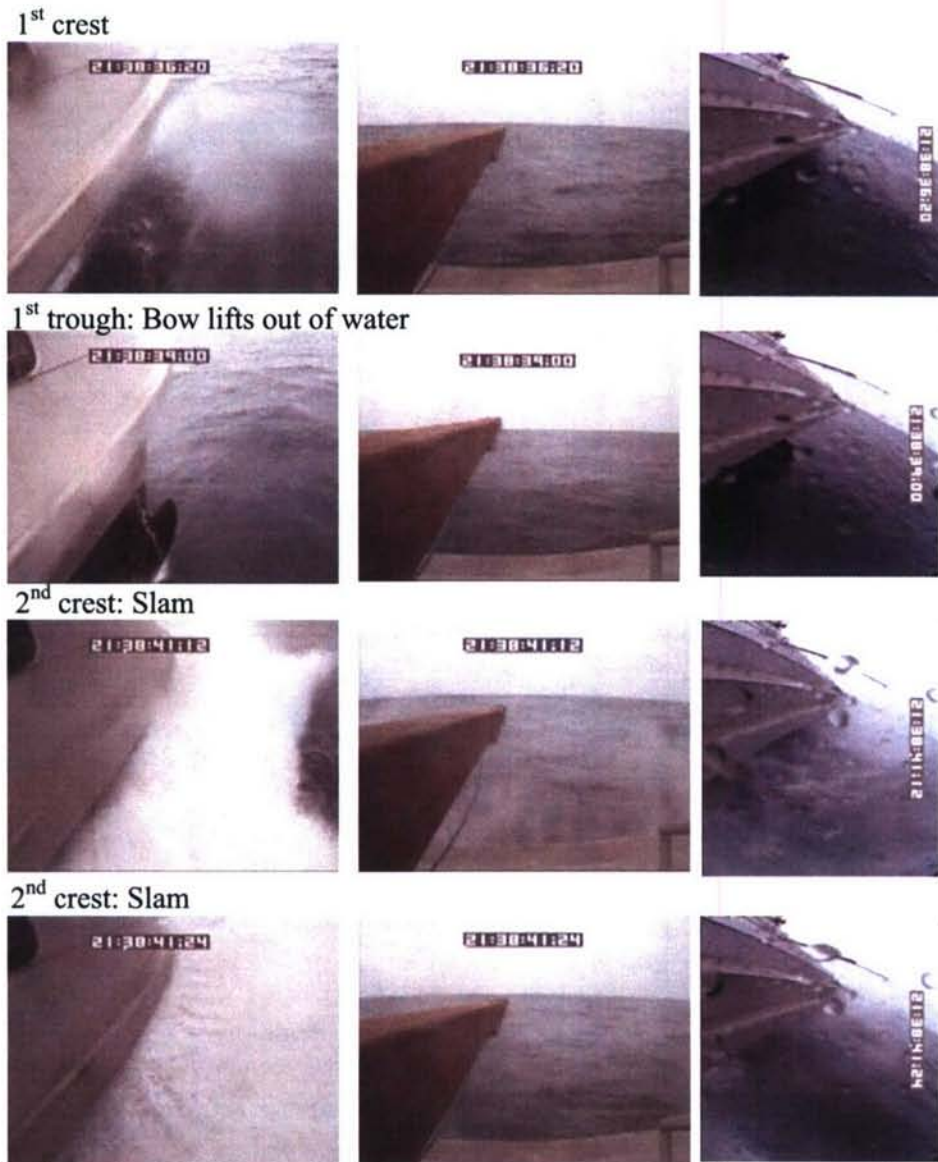

Figure 35. Slam Event 3B: Snapshots from on-board cameras.

The final slam is very similar to the first two. It also begins with a larger than average crest followed ay a trough that causes the bow to lift out of the water. The actual slam occurs as the ship encounters the second, and larger, crest which slams into the bottom of the hull in the center tunnel. Figure 36 shows this sequence of events.
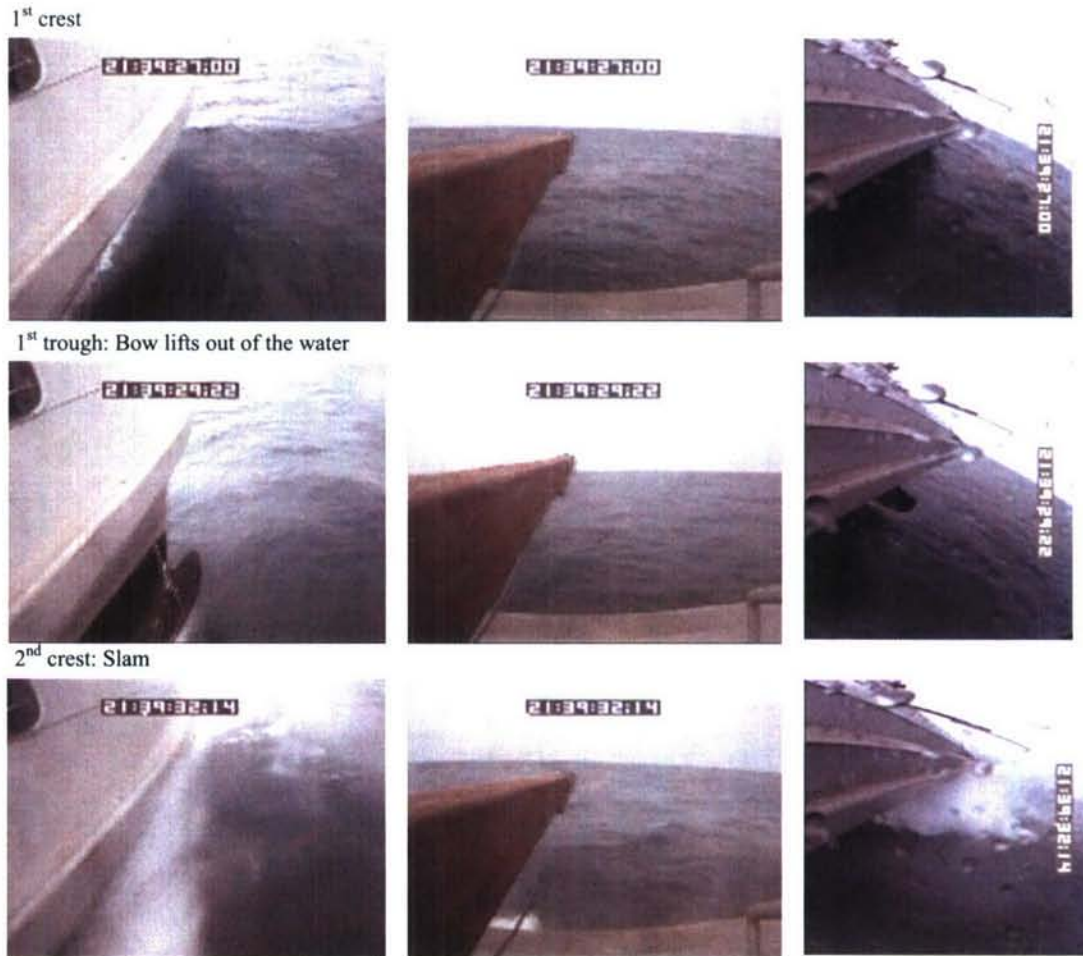
1st crest

1st trough: Bow lifts out of the water

2nd crest: Slam

Figure 36. Slam Event 3C: Snapshots from on-board cameras.

All three slams in this time period were caused by two consecutive wave crests that were significantly larger than the average wave height seen by the ship in the given time period. The second wave crest was the wave that caused the actual slam impact and it was always larger than the first crest and close to double the height of the average wave height envelope. In addition, during the wave trough between the two large wave crests the bow of the ship always lifted completely out of the water before the second crest slammed into the ship. During each trough in which the bow was out of the water the ship pitched above the 3 degree envelope and with each crest the bow pitched down below 0 degrees. The peaks in vertical acceleration accompanied the larger wave crests and the bow down pitch.

Figure 37 shows the sequence of events at about 21:37:40 GMT. The plot in Figure 33 indicates that this is a possible slam event since there are two consecutive wave crests greater than 10 ft which is similar to the trend seen in the three previously discussed slams. In addition, as shown by the snapshots in the second row of Figure 37, the wave trough after the first crest causes the bow of the ship to lift out of the water, also similar to the previous slams. However, the second crest is not large enough to make impact and cause a slam, explaining why no significant spike in vertical acceleration or pitch is seen. This is an example of a wave train that is close to the necessary conditions for a slam, but the wave crests are not large enough to cause ship motions outside of the average envelope.

1st crest

1st trough: Bow lifts out of the water

2nd crest: Not large enough to produce a slam
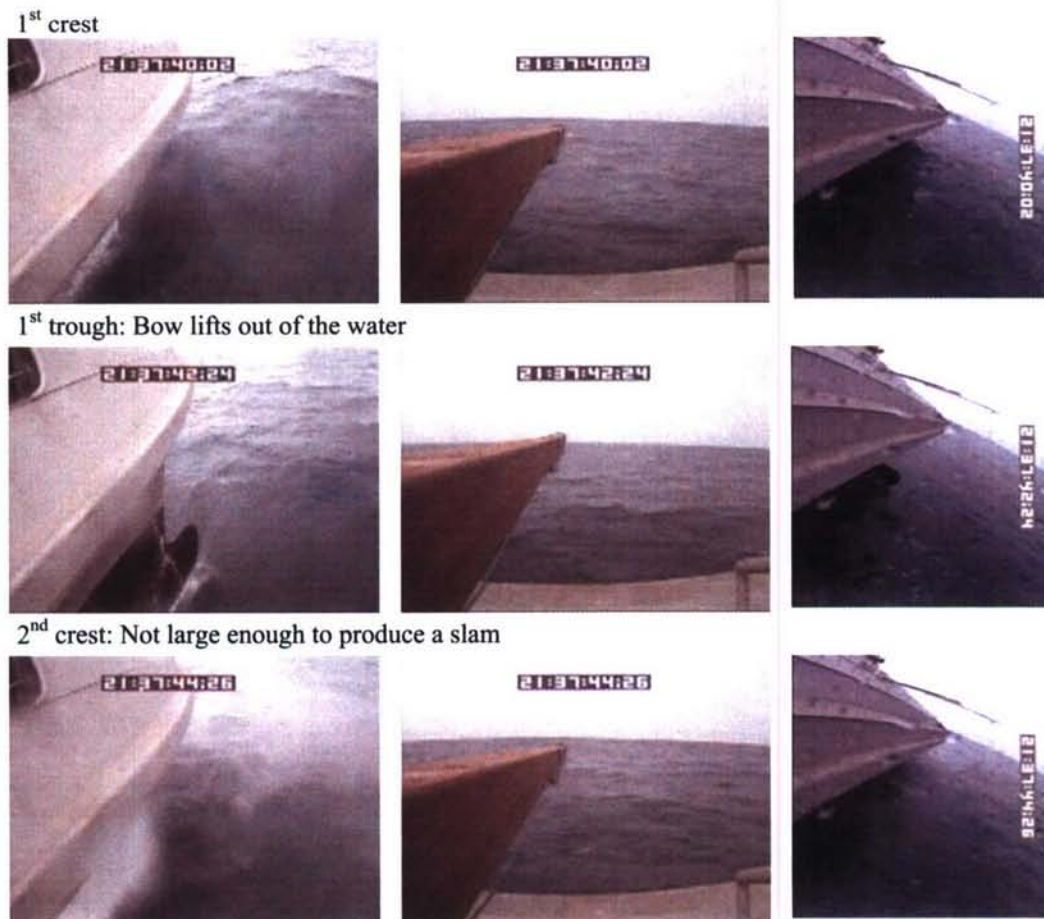
Figure 37. Slam Event 3: Snapshots of near-slam event.

Slam Event 4

Figure 38 provides wave height, pitch, and z linear acceleration plots for Slam Event 4. The spike in the z linear acceleration plot seen at approximately 22:08:45 GMT indicates the slam. Similar to Slam Event 3, Slam Event 4 has wave heights that on average stay within a ±10 ft range, pitch angles that stay within a 0 to 3 degree range and

vertical accelerations that fluctuate from ±0.2 g's. The event begins with a deep wave trough of about 15 ft, followed by a large 20 ft crest, another deep trough of more than 10 ft and a large crest of about 13 ft before the wave heights start to settle back into the ±10 ft envelope.

Figure 39 shows snapshots from the starboard, bow center, and starboard bowline cameras respectively during the slam event. With the first trough the bow lifts out of the water and with the following crest there is a slam impact. The bow then rises out of the water again with the second trough and the second crest also slams into the bow, this time more violently than the first as seen by the large amount of whitewater the cameras see and the sharp peak in vertical acceleration seen in Figure 38. With each trough the bow of the ship pitches upward, above the 3 degree boundary of the envelope and downward below zero degrees with each crest. The second crest, which causes the more violent slam, causes the greatest bow down pitch of -2 degrees that is seen which corresponds with the largest spike in vertical acceleration seen in Figure 38. Figure 40 shows a 30-second section of the plots shown in Figure 38 and illustrates how the ship's greatest bow down pitch corresponds with its maximum vertical acceleration.
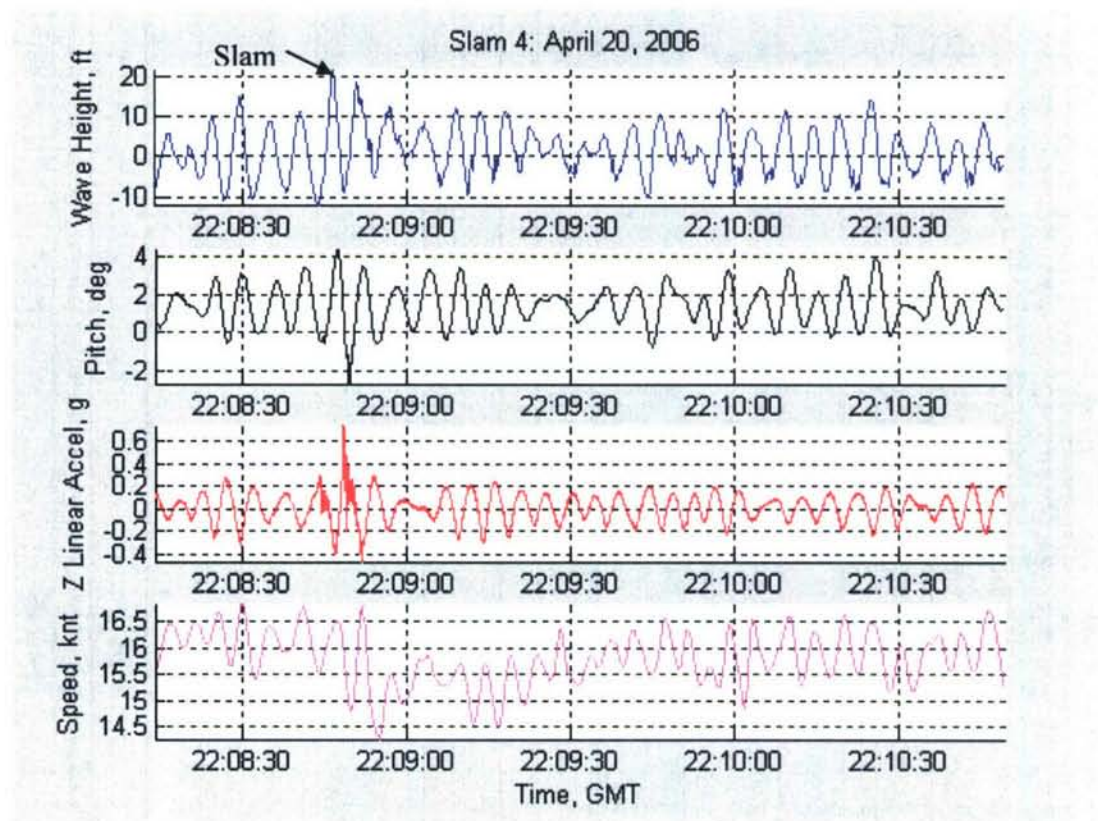

Figure 38. Slam Event 4: Wave Height, Pitch, Vertical Acceleration, and Speed plots.

1st trough: Bow lifts out of the water

1st crest: Slam

2nd trough: Bow lifts out of the water

2nd crest: 2nd and more violent slam

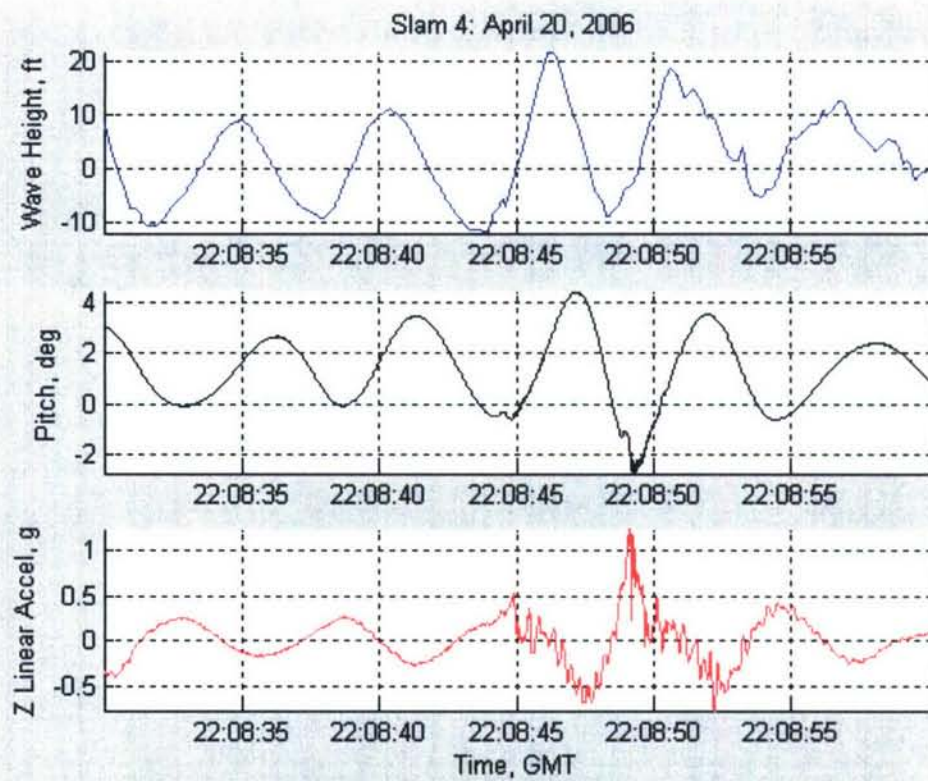Figure 39. Slam Event 4: Snapshots from on-board cameras.

Figure 40. Slam Event 4: 30 second close up plots of slam event.

CONCLUSIONS

Wave field and ship motions data were collected continuously during a four day trial from April 18-21, 2006 in the Pacific Northwest. From this data four high speed slam events were identified and then analyzed. A slam event was defined by the encounter of a wave large enough to make impact with and slam into the bottom of the ship's wetdeck. Slam events were most easily identified in the data by a large spike in the vertical linear acceleration of the ship. Three of the slam events analyzed occurred on the same day while the ship was traveling at 15-20 knots and the other slam event occurred the day before while traveling at a faster speed of 30 knots.

All four slam events had similar characteristics. For the three time periods analyzed on the same day the wave heights seen by the ship stayed within a ±10 ft envelope before and after the slam. For the other slam the wave height envelope was ±5 ft. In addition, pitch fluctuated within a 0 to 2 or 3 degree range and the vertical acceleration oscillated between ±0.2 g's. The actual slams were caused by waves that were larger than the given envelope and caused ship motions outside of the average range of motion. Each slam involved at least two consecutive wave crests larger than the average envelope and the bow of the ship always lifted out of the water during the trough before the crest that caused the most intense slam. The strength of the slam was determined by the magnitude of the vertical acceleration. The greater the spike in the z linear acceleration above the ±0.2 g envelope the stronger or more violent was the slam. The second large crest always caused a slam, however sometimes both crests had a slam impact. In the case of Slam Event 2 both crests caused a weak slam causing an increase of only 0.2 g's above the ±0.2 g envelope to a total vertical acceleration of 0.4 g's. Slam Events 1 and 4 also had slams occur with each wave crest however the second crest caused a much more violent slam than the first leading to over an 0.8 g vertical acceleration in both cases.

During each wave trough the bow of the ship pitched upwards, sometimes as high as 4 degrees. The greatest amount of pitch was usually with the trough following the most intense slam. In addition, during each crest the bow pitched downward with the maximum downward pitch angle (-2 degrees) corresponding to the crest that caused the strongest slam. This largest change in pitch that was always seen with the impact of the second slamming wave crest also corresponded with the largest change in vertical linear acceleration. The height of the wave crest that caused the slam impact was often twice the height of the average wave height envelope.

Overall, it can be concluded that for the cases analyzed two consecutive wave crests larger than the average wave height envelope were necessary to cause a slam event. The crest that caused the slam had to be at least 50% larger than the upper bound of the wave height envelope. In addition, it was seen that during the troughs before a slamming crest the bow of the ship lifted out of the water. With each slam impact the ship pitched down below the lower boundary of the pitch envelope and pitched up above the envelope with each crest.

ACKNOWLEDGEMENTS

THIS PAGE INTENTIONALLY LEFT BLANK

APPENDIX A

TSK Shipborn Wave Height Meter

The TSK Wave Height Meter is a shipboard instrument designed to measure wave heights and periods. The system consists of a sensor unit, accelerometer, connections box, and a signal processor. The sensor is mounted directly above the waves to be measured and uses microwaves to detect its target. It has a wave height range of ±14.5 m, resolution of 1.4 cm and a period range of 0 to 20 seconds and its data includes a Doppler shift due to the sea surface motion. The accelerometer removes ship motion from the amplitude measurements and the signal processor converts the raw data it receives from the connections box into a useable form. It integrates the Doppler motion data to obtain wave amplitude data and double integrates the accelerometer data to determine vertical ship motion. The ship motion is then subtracted from the processed sensor data to determine the actual wave amplitude.

Neptune Buoy

This buoy is a Wave Sentry Buoy originally developed by Neptune Sciences Inc, (now a part of Planning Systems Inc). The Neptune buoy provides users with real-time directional and non-directional wave data. Processed data includes wave height, wave period, and wave direction as well as both non-directional and directional wave spectra. The buoy has a sampling rate of 4 Hz and recording period of 17.1 minutes.

NOAA Buoy 46087 and 46028

These buoys are part of the NOAA Marine Environmental Buoy Database that is managed by the National Oceanographic Data Center (NOCD). The buoys collect and report wave data (wave height, wave period, and wave spectra) that is received monthly by NOCD. All data is made available online at NOCD's website: http://www.nodc.noaa.gov.

THIS PAGE INTENTIONALLY LEFT BLANK
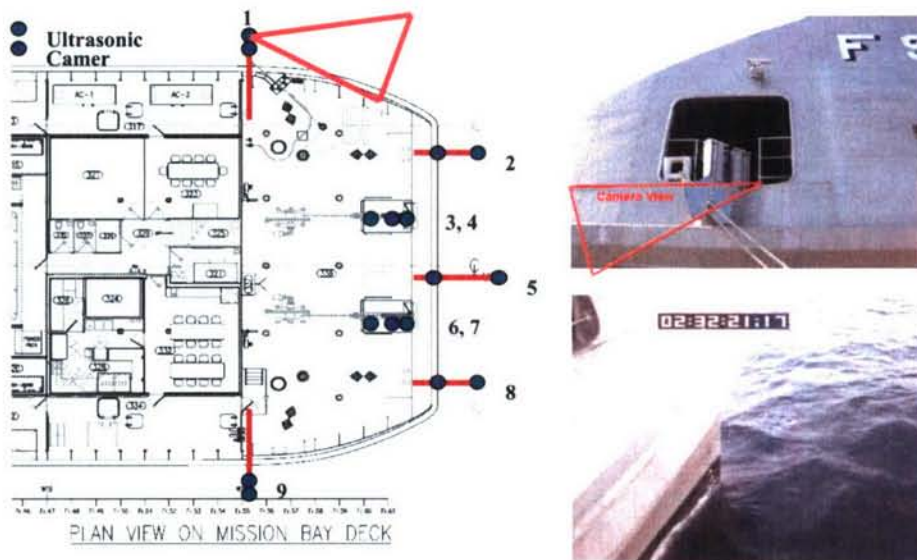
APPENDIX B

Underway Camera Views

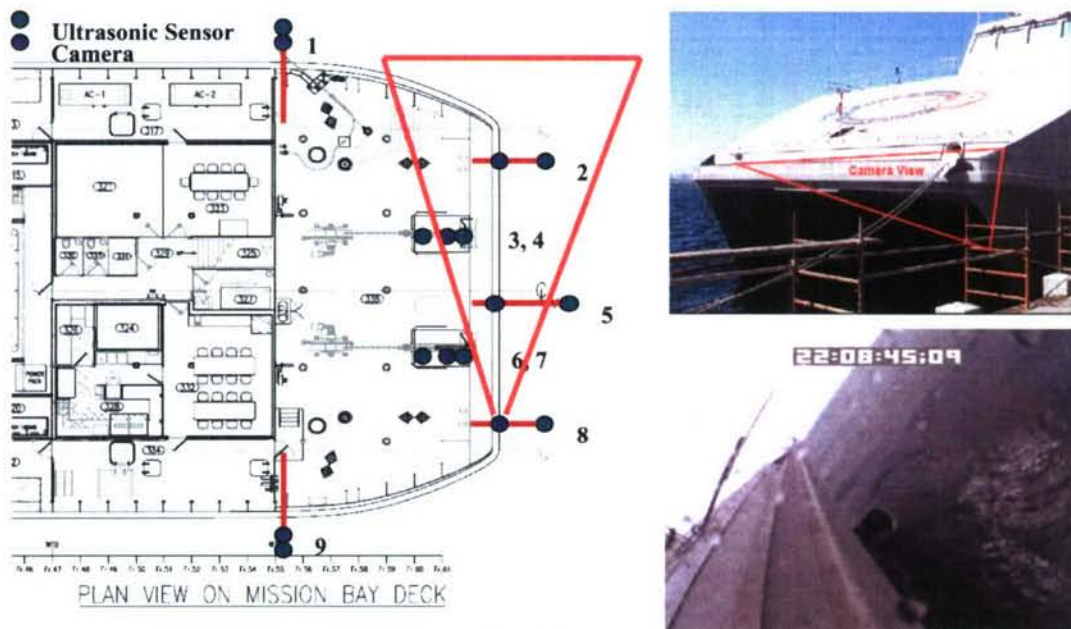Figure B1. Diagram of view from port bow camera.

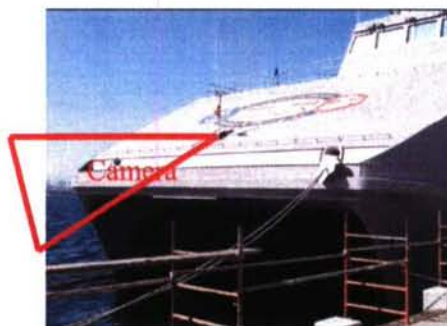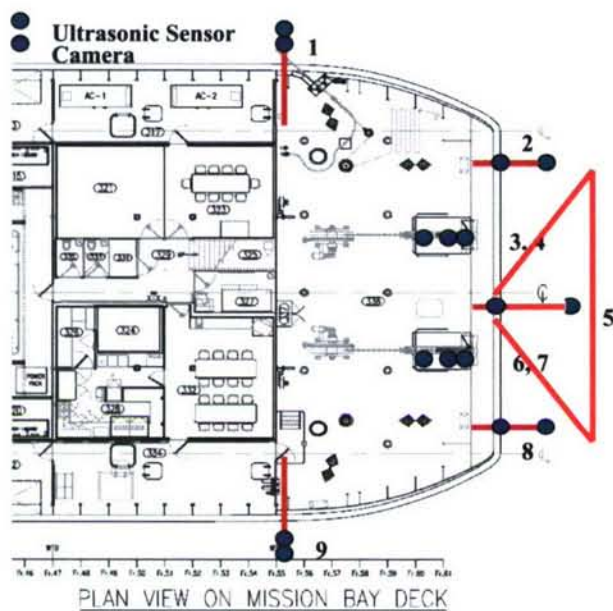Figure B2. Diagram of view from starboard bowline camera.

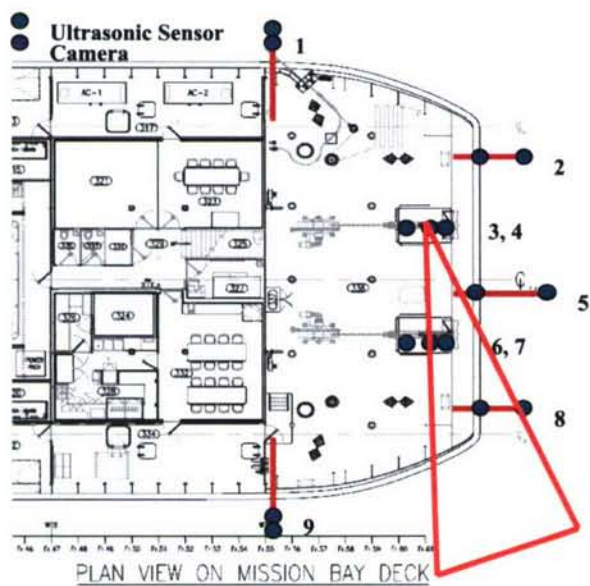Figure B3. Diagram of view from center bow camera.
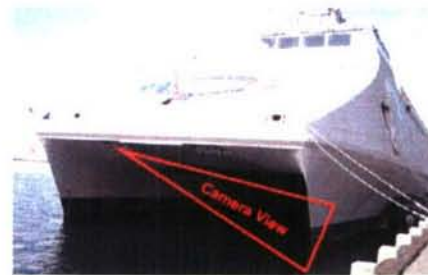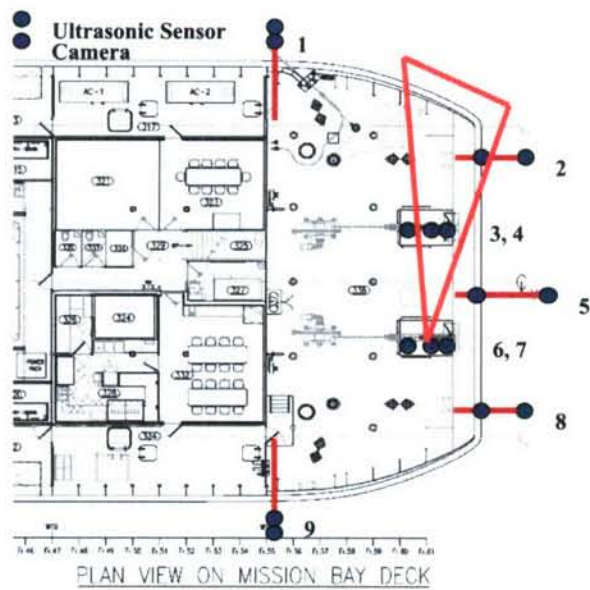

Figure B4. Diagram of view from port anchor well camera.

Figure B5. Diagram of view from starboard anchor well camera.

THIS PAGE INTENTIONALLY LEFT BLANK

APPENDIX C

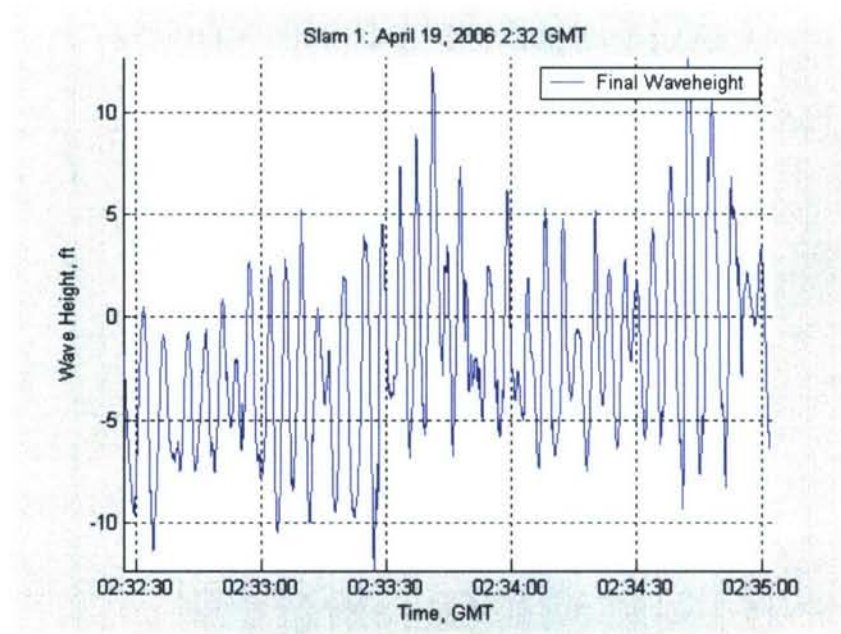## Wave Field Characterization for Slam Events

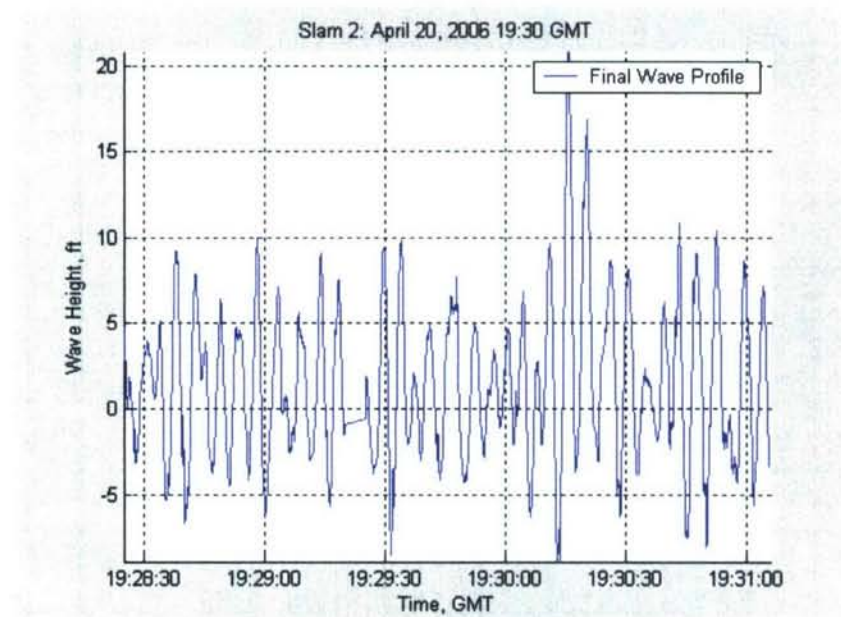Figure C1. Slam Event 1: Final Wave Profile.
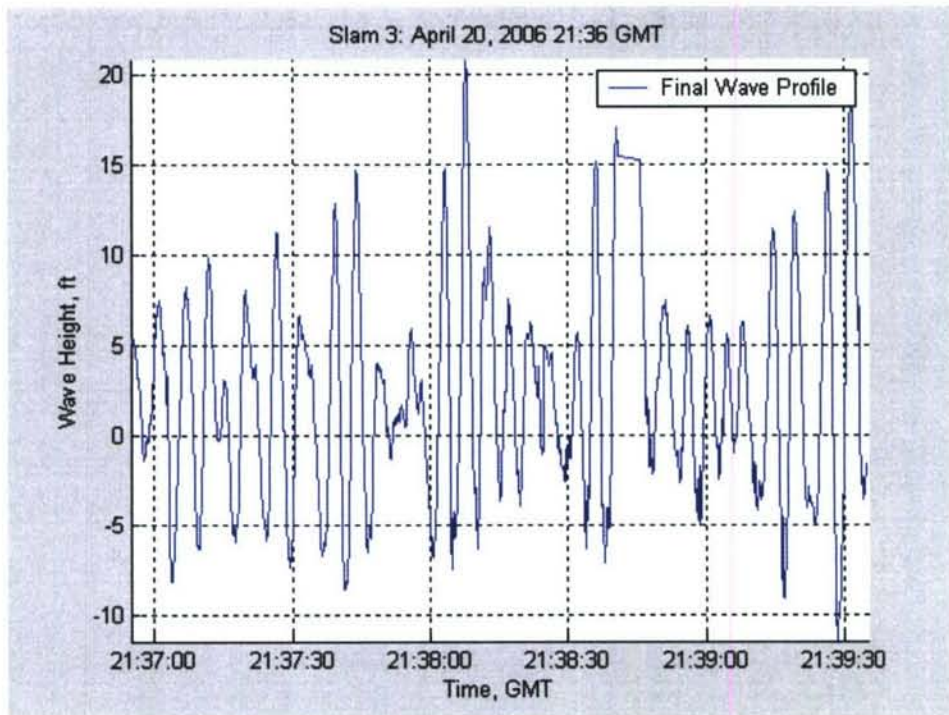

Figure C2. Slam Event 2: Final Wave Profile.

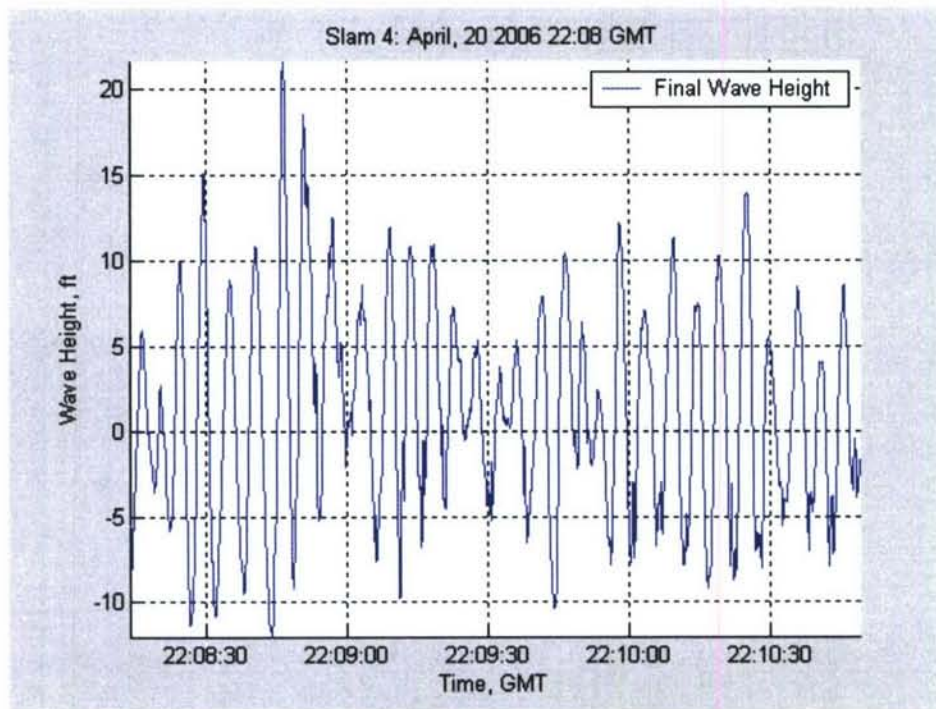Figure C3. Slam Event 3: Final Wave Profile.

Figure C4. Slam Event 4: Final Wave Profile.

50

DISTRIBUTION

Copies
1   DTIC

ONR
1   331   P.Purtell

DIVISION DISTRIBUTION
1   3452   Library
1   5010 ff (w/o enclosure)
1   5060   D. Walden
1   5200   D. Walker
1   5400   M. Donnelly
1   5500   B. Bachman
1   5600   T. Fu, A. Fullerton, L. Minnick, K. Anderson (w/o enclosure)
1   6530   T. Brady